associated with the RE1 and RE2 p53-response elements of the p21 promoter, but not with an unrelated region of p21 (Fig. 3*D*). Knockdown of MOZ expression by pretreatment of MCF-7 cells with a MOZ-specific siRNA partially inhibited the recruitment of p53 to the p21 promoter by DNA damage, but not MDM2, Bax, and Puma (Fig. 3*E*, and supplemental Fig. S3, *H–J*). Furthermore, binding of MOZ to the p21 promoter was detected in $p53^{+/+}$ HCT116 cells but not in $p53^{-/-}$ HCT116 cells (Fig. 3*F*). Thus, these results suggest that the p53-MOZ interaction is involved in recruitment to and activation of the p21 gene promoter, and that the recruitment of the p53-MOZ complex to the p21 promoter is p53 dependent.

Increase in the Level of the p53-MOZ Complex in Response to DNA Damage—To test interactions between endogenous p53 and MOZ proteins, levels of MOZ, as well as p300, in p53 immunoprecipitates were monitored in γ irradiation-exposed MCF-7 cells. A p53-MOZ complex was nearly undetected in non-irradiated cells, but appeared following irradiation of MCF-7 cells and reached a maximum at 2 h (Fig. 4*A*). An increase in p53-p300 complex was also observed after irradiation. Immunoblot analysis indicated that these increases were associated with increases in overall p53 protein level, as well as in p53 phosphorylation on Ser^{15}, and were followed by an increase in p21 expression. These results indicate that p53 interacts with MOZ in response to DNA damage.

Post-translational Modification of p53 Correlates with p53-MOZ Interaction—p53 is stabilized and activated upon DNA damage primarily through post-transcriptional modifications including phosphorylation and acetylation (14–19, 22, 41–43). Differential modifications of p53 may be important for differential activation of target genes (44–46). To test the effects of such modifications on p53 interactions, we performed co-immunoprecipitation analysis using p53 mutant proteins, in which potential modification sites were altered. Interaction of p53 with MOZ was impaired by mutation of Ser^{15} to Ala (S15A) and Ser^{20} to Ala (S20A) (Fig. 4*B*). In contrast, the p53-MOZ interaction was enhanced by mutation of Ser^{15} to Asp (S15D) and Ser^{20} to Asp (S20D), which mimic serine phosphorylation. However, mutation of Ser^{46} to Asp (S46D) showed defects in enhancement of the interaction. These results indicate that phosphorylation of p53 on Ser^{15} and Ser^{20} enhances its interaction with MOZ. Furthermore, substitution of the major acetylation site (Lys^{382}) with Arg (K382R) strongly enhanced the p53-MOZ interaction, but not K382Q (Fig. 4*B*), suggesting that Lys^{382} acetylation also plays an important role in the p53-MOZ interaction. These results suggest that the interaction between p53 and MOZ correlates with specific post-translational modifications, such as phosphorylation and acetylation.

p53-MOZ Complex Is Associated with p21 Expression—To further investigate this hypothesis, we compared interactions of p53-MOZ and p53-p300 following various doses of UV irradiation in MCF-7 cells. Levels of the p53-p300 complex increased in a dose-dependent manner (Fig. 4*C*). In contrast, levels of the p53-MOZ complex increased after MCF-7 cells irradiation of 30 J/m², but not 50 J/m². The lower irradiation dose was correlated with induction of p21 expression and G_1 arrest (Fig. 4, *C* and *D*). Thus these results suggest that interactions of p53-MOZ and p53-p300 are differentially regulated, and that the

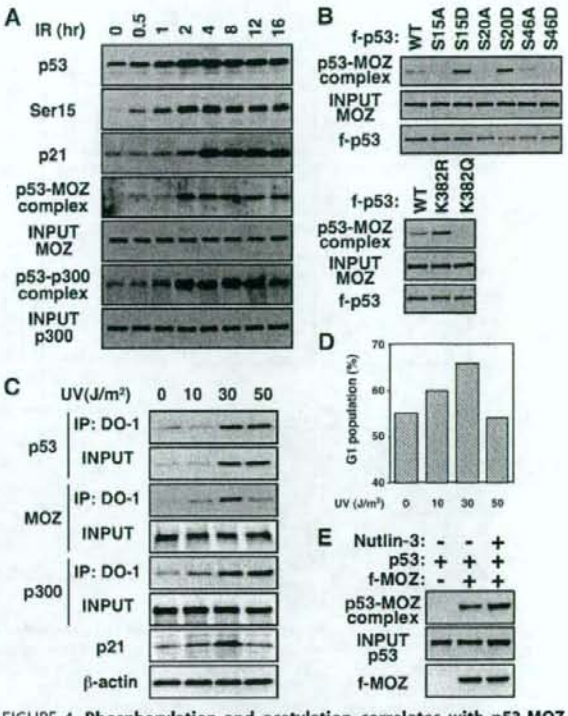

FIGURE 4. **Phosphorylation and acetylation correlates with p53-MOZ complex formation.** *A*, both p53-MOZ and p53-p300 complexes were formed over time following γ irradiation (*IR*, 10 gray) of MCF-7 cells. Cell lysates were immunoblotted using anti-p53, anti-phospho (Ser^{15})-p53, or anti-p21 antibodies. p53-MOZ and p53-p300 complexes were detected by immunoprecipitation using an anti-p53 antibody (*DO-1*). The immunoprecipitates (p53-MOZ-p300 complex) and input lysates (*INPUT MOZ/p300*) were subjected to immunoblot analysis using anti-MOZ or anti-p300 antibodies to detect complex formation with p53. *B*, Bosc 23 cells were transfected with the indicated FLAG-tagged wild-type (*WT*) or mutant (S15A, S15D, S20A, S20D, S46A, S46D, K382R, or K382Q) of p53 together with HA-tagged MOZ. Cell lysates were immunoprecipitated with anti-FLAG M2 affinity beads and subjected to immunoblot analysis using anti-HA or anti-FLAG antibodies to detect p53-MOZ complexes or p53, respectively. Input lysate samples were subjected to immunoblot analysis using anti-HA antibody (*INPUT MOZ*). *C*, complex formation of p53-MOZ and p53-p300 and expression of p21 after the indicated doses of UV radiation in MCF-7 cells. Complexes were detected by immunoprecipitation with anti-p53 antibody (*IP: DO-1*), followed by immunoblot analysis using anti-p53, anti-MOZ, or anti-p300 antibodies. Input lysate samples (*INPUT*) were subjected to immunoblot analysis using anti-p53, anti-MOZ, anti-p300, anti-p21, or anti-β-actin (loading control) antibodies. *D*, fluorescence-activated cell sorter analysis after UV radiation. The G_1 population in MCF-7 cells was analyzed at 24 h following exposure to the indicated doses of UV radiation. *E*, the amount of p53 correlates with p53-MOZ complex formation. Bosc 23 cells were co-transfected with FLAG-tagged MOZ (*f-MOZ*) together with HA-tagged p53, as indicated. At 24 h after transfection, the cells were treated with or without 20 μM Nutlin-3 for 6 h. The cell lysates were immunoprecipitated with anti-FLAG M2 affinity beads and subjected to immunoblot analysis using the anti-HA (*p53-MOZ complex*) or anti-FLAG (*f-MOZ*) antibodies. Input lysates were partially subjected to immunoblot analysis using anti-HA (*INPUT p53*) antibody.

p53-MOZ complex is associated with p21 expression and induction of G_1 arrest.

Oncogenic G279E Mutation Inhibits the p53-MOZ Interaction—Mutations in p53 are frequently found in human cancers. Although ~1400 different p53 mutations have been reported, the large majority of mutations are located in the core domain that is essential for binding to specific DNA sequences (47, 48), suggesting that impaired interaction of p53 with DNA

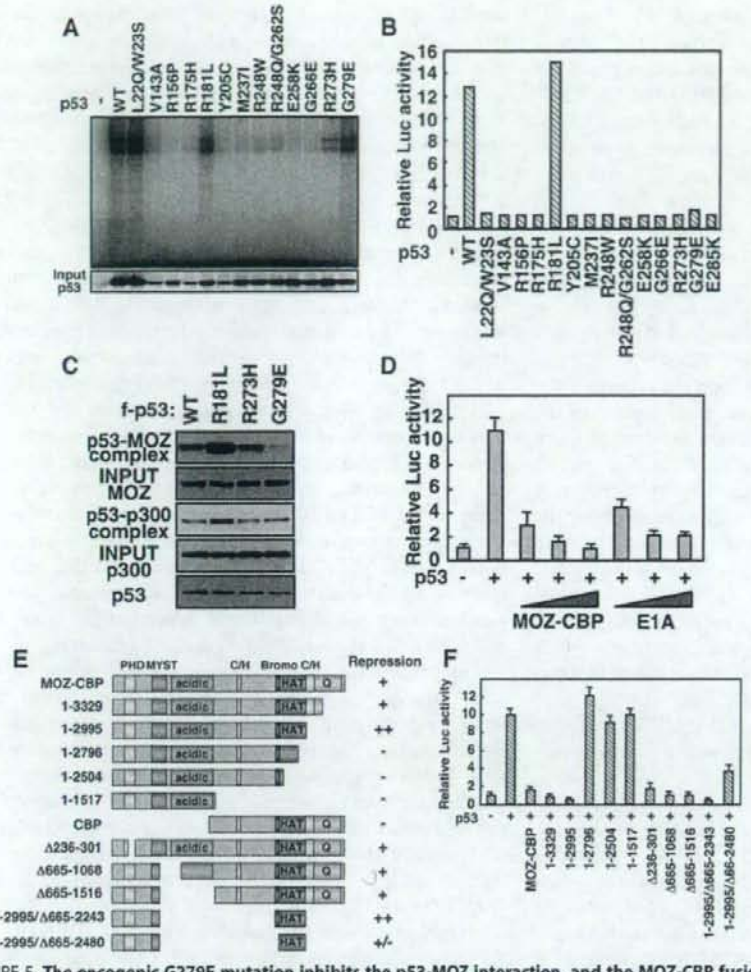

FIGURE 5. **The oncogenic G279E mutation inhibits the p53-MOZ interaction, and the MOZ-CBP fusion protein inhibits p53-mediated transactivation.** *A*, DNA binding assay of somatic mutants *versus* wild-type (*WT*) p53. WT and indicated mutants of p53 were incubated with a ^{32}P-labeled wild-type p21 oligonucleotide, subjected to electrophoresis, and visualized by autoradiography. The expression level of transfected p53 is shown in the *bottom panel* (*Input p53*). *B*, effects of previously reported somatic p53 mutants on transcription of p21. Saos-2 cells were transfected with 50 ng of p21-luc (*lanes 1–16*), 200 ng of WT or mutant pLNCX-*p53* (*lanes 2–16*), and pRL-CMV as a control for transfection efficiency. Luciferase assays were performed 24 h post-transfection. *C*, effects of p53 mutants on interaction with MOZ. Bosc 23 cells were transfected with FLAG-tagged WT or mutant (R181L, R273H, or R279E) of *p53* together with HA-tagged *MOZ/p300*. Cell lysates were immunoprecipitated with anti-FLAG M2 affinity beads and subjected to immunoblot analysis using anti-HA or anti-FLAG antibodies to detect the p53-MOZ/p300 complex and p53, respectively. Input lysate samples were subjected to immunoblot analysis using anti-HA antibody (*INPUT MOZ/p300*). *D*, MOZ-CBP inhibits p53-mediated transcription. Saos-2 cells were transfected with 50 ng of *p21*-luc, 10 ng of pLNCX-*p53* (*lanes 2–8*) and 30 (*lane 3* and *6*), 100 (*lanes 4* and *7*), or 350 ng (*lanes 5* and *8*) *MOZ-CBP* or *E1A*, and 25 ng of pRL-CMV as a control for transfection efficiency. Luciferase assays were performed 24 h post-transfection. *E*, schematic representation of the structure of MOZ-CBP deletion mutants used for determining the p53 interacting domains. The PHD-type zinc finger domain (*PHD*), acidic domain (*acidic*), bromo domain (*Bromo*), HAT, Cys/His-rich domain (*C/H*), and Glu-rich domain (*Q*) are indicated. *F*, effects of MOZ-CBP deletion mutants on p53 activity. Saos-2 cells were transfected with 50 ng of *p21*-luc (*lanes 1-13*), 200 ng of pLNCX-*p53* (*lanes 2-13*), 350 ng of pLNCX-HA-*MOZ-CBP* mutants (*lanes 3-13*) and 25 ng of pRL-CMV. Luciferase assays were performed 24 h post-transfection.

is associated with cancer. In fact, most of these mutations in the core domain abolish p53 DNA binding and activation of transcription (Fig. 5, *A* and *B*). The G279E mutant, however, lacks the ability to activate transcription, but still has the ability to bind DNA. The MOZ-interacting domains also map to the p53 core domain (Fig. 1*D* and supplemental S2); therefore, we tested the interaction of this G279E mutant with MOZ, and found that the G279E mutant is unable to bind MOZ (Fig. 5*C*).

A MOZ-CBP fusion gene is produced by the t(8;16) translocation associated with acute monocytic leukemia. We tested the effects of MOZ-CBP on p53-dependent transcription, and found that the MOZ-CBP fusion protein, as well as adenovirus E1A, strongly inhibited p53-dependent transcription of *p21* in a dose-dependent manner (Fig. 5*D*). Deletion analysis showed that the bromo and HAT domains in the CBP region of the fusion protein are important for MOZ-CBP inhibition of p53-mediated transcription (Fig. 5, *E* and *F*).

DISCUSSION

The data presented here demonstrate that MOZ, a MYST-type histone acetyltransferase, directly interacts with p53, and that the interaction is regulated by phosphorylation and acetylation. Like other co-factors, such as p300/CBP and PCAF, MOZ functions as a co-activator of p53. However, MOZ stimulates p53-mediated transcription of p21 to induce cell-cycle arrest, but not other p53 target genes, such as Bax or AIP1. We partially purified MOZ complexes from transfected Bosc 23 cells that transiently expressed FLAG-tagged MOZ. Mass spectrometry and IP immunoblot analyses revealed that MOZ could interact with p53. In contrast with previous reports in which levels of the p53-p300 or p53-CBP interaction increased in a dose-dependent manner with increasing DNA damage (16, 18, 19), levels of the p53-MOZ complex increased with levels of DNA damage to induce cell-cycle arrest (Fig. 4*C*).

Among the most distinctive features of p53 is the ability to induce either cell-cycle arrest or apoptotic death. Although this differential activity may be partially explained by the molecular mechanisms of promoter discrimination, the precise mechanism of the selective activation of p53 target genes remains

unknown. In response to severe DNA damage, MYST acetyltransferases, such as TIP60 and MOF, acetylate Lys^{120} of p53. This acetylation results in preferential accumulation of p53 on proapoptotic promoters, such as Bax and PUMA (50, 52). CAS/CSE1L, which suppresses histone H3K27 methylation, selectively associates with the PIG3 and AIP1 promoters, but not the p21 promoter (12). In addition, Hzf, which is a p53 target gene, interacts directly with the p53 DNA binding domain, and induces preferential expression of p53 target genes that block the cell cycle, such as p21 and 14-3-3σ (10).

In this report, we demonstrated that MOZ could interact with p53 and that the p53-MOZ complex increases p21 expression in cells exposed to doses of DNA damage that induce cell-cycle arrest. In response to DNA damage, p53 is phosphorylated on Ser^{15} and Ser^{20} to recruit MOZ, and subsequently the p53-MOZ complex preferentially induces transcription of the cell cycle-related p21 gene. The interaction between p53 and MOZ is regulated by post-translational modification, such as phosphorylation and acetylation, of N- and C-terminal residues of p53, respectively (Fig. 4*B*). In addition, deletion of either the N- or C-terminal of p53 enhances its interaction with MOZ (supplemental Fig. S2). These results suggest that the MOZ-binding domain of p53 is masked by its N- and C-terminal domains and that post-translational modifications, such as phosphorylation and acetylation, of N- and C-terminal regions of p53 have an effect on its conformation to regulate interactions with MOZ. Furthermore, p53-MOZ interaction was also slightly affected by Nutlin-3, the antagonist of MDM2, suggesting that the stabilization of p53 is also important for regulation of p53 and MOZ interaction (Fig. 4*E*) (49, 50).

ChIP analysis and reporter analysis showed that DNA damage could induce recruitment of the p53-MOZ complex to the p21 promoter. Experiments using $MOZ^{-/-}$ MEFs revealed that MOZ-deficient cells failed to arrest in the G_1 phase in response to DNA damage and were more sensitive to DNA damage. As shown by immunoblot and RT-PCR analyses, the expression of p21 was profoundly impaired in $MOZ^{-/-}$ MEFs after ADR treatment (Fig. 3, *A* and *B*, supplemental Fig. S3, *A–C*). These results suggest that MOZ stimulates p53-dependent transcription of the $p21^{Waf1}$ gene, thereby regulating cell-cycle arrest.

$MOZ^{-/-}$ mice die at around embryonic day 15 (E15) (33). The response of $MOZ^{-/-}$ MEFs to DNA damage suggests that the p53 pathway may be altered in $MOZ^{-/-}$ MEFs. In fact, induced expression of p21 was profoundly impaired in $MOZ^{-/-}$ MEFs as assessed by immunoblot and RT-PCR analyses.

A previous report demonstrated that p21 expression was not induced in $p53^{-/-}$ cells after ADR treatment, and Bax expression was only slightly affected (51). DNA damage-induced cell-cycle arrest was impaired in $MOZ^{-/-}$ MEFs (Fig. 2*A*), as observed in p53-null and p21-null cells. These results suggest that the enhanced apoptosis found in $MOZ^{-/-}$ MEFs may be due to reduced induction of p21 and impaired cell-cycle arrest. In fact, reporter analysis indicated that MOZ did not increase the activity of the Bax and AIP1 promoters (supplemental Fig. S3, *F* and *G*). Although the specific expression mechanisms are currently unknown, there are two possibilities. Because the p53-MOZ complex prefers the p21 promoter to other promoters (Fig. 3*D*), formation of the p53-MOZ complex may inhibit transcription of apoptotic genes by reducing levels of available p53. Alternatively, MOZ may enhance p53-mediated cell-cycle arrest, thereby inhibiting transcription of apoptotic genes indirectly. $p300^{-/-}$ MEFs retain the ability to respond to UV irradiation by stabilization of p53 and induction of p21 (52). Because CBP functions as a co-activator to p53 as well as p300, CBP may compensate for p300 function in $p300^{-/-}$ MEFs.

Somatic mutations in p53 are found in ~50% of all human cancers. Approximately 1400 different p53 mutations have been reported, with the large majority of such mutations located in the DNA binding core domain (47, 48). Domain analysis using p53 deletion mutants indicated that the DNA-binding core domain of p53 is required for interactions with MOZ, which suggests that the p53-MOZ complex controls access of p53 to binding sites in target gene promoters and that MOZ may play a role in the selectivity of p53-mediated activation of transcription. In the process of screening somatic tumor-associated p53 mutants, we found that the G279E mutation of p53, which did not affect DNA binding to p53 responsive elements but impaired transcription of p21, disrupted the interaction between p53 and MOZ. These results suggest that MOZ functions as a co-activator of p53, and that activation of p53-dependent transcription of p21 may depend on the interaction of p53 with MOZ to recruit p53 to the p21 promoter.

The MOZ-CBP leukemic fusion gene is produced by the t(8,16) translocation, which is associated with acute myeloid leukemia, suggesting that MOZ-CBP may affect the growth and differentiation of hematopoietic cells. We found that the MOZ-CBP fusion protein inhibits p53-mediated transactivation of p21 (Fig. 5, *D* and *F*). Because MOZ-CBP fusion protein showed reduced activity for acetylation of p53 as compared with either CBP or MOZ alone, MOZ-CBP might suppress p53 acetylation by competing with other HAT protein such as CBP and MOZ (supplemental Fig. S4, *A* and *B*).

Another leukemia-associated fusion, MOZ-TIF2, also inhibits p53-dependent transcription (37). ChIP analysis indicated that MOZ-CBP directly inhibits binding of p53 to the p21 promoter (supplemental Fig. S4*C*). These results suggest that p53 dysfunction associated with MOZ gene translocations and inhibition of p53/MOZ-mediated transcription are involved in the pathogenesis of leukemia and other cancers.

Acknowledgments—We thank Dr. D. M. Livingston for p300 cDNA, Dr. D. Baltimore for Bosc 23 cells, Dr. H. Arakawa for MCF-7 cells, Ad-p53, and AdCaLacZ, and Dr. M. Enari for p21 cDNA and GST-p53. We also thank Drs. H. Ichikawa, K. Yamagata, and A. Taniyama for helpful discussions, and S. Mitani for technical assistance.

REFERENCES

1. Harris, S. L., and Levine, A. J. (2005) *Oncogene* **24,** 2899–2908
2. Vousden, K. H., and Lu, X. (2002) *Nat. Rev. Cancer* **2,** 594–604
3. el-Deiry, W. S., Tokino, T., Velculescu, V. E., Levy, D. B., Parsons, R., Trent, J. M., Lin, D., Mercer, W. E., Kinzler, K. W., and Vogelstein, B. (1993) *Cell* **75,** 817–825
4. Miyashita, T., and Reed, J. C. (1995) *Cell* **80,** 293–299
5. Nakano, K., and Vousden, K. H. (2001) *Mol. Cell* **7,** 683–694
6. Lane, D. P. (1992) *Nature* **358,** 15–16
7. Levine, A. J. (1997) *Cell* **88,** 323–331

8. Michael, D., and Oren, M. (2002) *Curr. Opin. Genet. Dev.* **12,** 53–59
9. Prives, C., and Hall, P. A. (1999) *J. Pathol.* **187,** 112–126
10. Das, S., Raj, L., Zhao, B., Kimura, Y., Bernstein, A., Aaronson, S. A., and Lee, S. W. (2007) *Cell* **130,** 624–637
11. Sykes, S. M., Mellert, H. S., Holbert, M. A., Li, K., Marmorstein, R., Lane, W. S., and McMahon, S. B. (2006) *Mol. Cell* **24,** 841–851
12. Tanaka, T., Ohkubo, S., Tatsuno, I., and Prives, C. (2007) *Cell* **130,** 638–650
13. Tang, Y., Luo, J., Zhang, W., and Gu, W. (2006) *Mol. Cell* **24,** 827–839
14. Giaccia, A. J., and Kastan, M. B. (1998) *Genes Dev.* **12,** 2973–2983
15. Gu, W., and Roeder, R. G. (1997) *Cell* **90,** 595–606
16. Lambert, P. F., Kashanchi, F., Radonovich, M. F., Shiekhattar, R., and Brady, J. N. (1998) *J. Biol. Chem.* **273,** 33048–33053
17. Shieh, S. Y., Ahn, J., Tamai, K., Taya, Y., and Prives, C. (2000) *Genes Dev.* **14,** 289–300
18. Dumaz, N., and Meek, D. W. (1999) *EMBO J.* **18,** 7002–7010
19. MacPherson, D., Kim, J., Kim, T., Rhee, B. K., Van Oostrom, C. T., DiTullio, R. A., Venere, M., Halazonetis, T. D., Bronson, R., De Vries, A., Fleming, M., and Jacks, T. (2004) *EMBO J.* **23,** 3689–3699
20. Thut, C. J., Chen, J. L., Klemm, R., and Tjian, R. (1995) *Science* **267,** 100–104
21. Ito, M., Yuan, C. X., Malik, S., Gu, W., Fondell, J. D., Yamamura, S., Fu, Z. Y., Zhang, X., Qin, J., and Roeder, R. G. (1999) *Mol. Cell* **3,** 361–370
22. Sakaguchi, K., Herrera, J. E., Saito, S., Miki, T., Bustin, M., Vassilev, A., Anderson, C. W., and Appella, E. (1998) *Genes Dev.* **12,** 2831–2841
23. Candau, R., Scolnick, D. M., Darpino, P., Ying, C. Y., Halazonetis, T. D., and Berger, S. L. (1997) *Oncogene* **15,** 807–816
24. Barlev, N. A., Liu, L., Chehab, N. H., Mansfield, K., Harris, K. G., Halazonetis, T. D., and Berger, S. L. (2001) *Mol. Cell* **8,** 1243–1254
25. Espinosa, J. M., Verdun, R. E., and Emerson, B. M. (2003) *Mol. Cell* **12,** 1015–1027
26. Borrow, J., Stanton, V. P., Jr., Andresen, J. M., Becher, R., Behm, F. G., Chaganti, R. S., Civin, C. I., Disteche, C., Dube, I., Frischauf, A. M., Horsman, D., Mitelman, F., Volinia, S., Watmore, A. E., and Housman, D. E. (1996) *Nat. Genet.* **14,** 33–41
27. Chaffanet, M., Gressin, L., Preudhomme, C., Soenen-Cornu, V., Birnbaum, D., and Pebusque, M. J. (2000) *Genes Chromosomes Cancer* **28,** 138–144
28. Kitabayashi, I., Aikawa, Y., Yokoyama, A., Hosoda, F., Nagai, M., Kakazu, N., Abe, T., and Ohki, M. (2001) *Leukemia* **15,** 89–94
29. Carapeti, M., Aguiar, R. C., Goldman, J. M., and Cross, N. C. (1998) *Blood* **91,** 3127–3133
30. Liang, J., Prouty, L., Williams, B. J., Dayton, M. A., and Blanchard, K. L. (1998) *Blood* **92,** 2118–2122
31. Bristow, C. A., and Shore, P. (2003) *Nucleic Acids Res.* **31,** 2735–2744
32. Kitabayashi, I., Aikawa, Y., Nguyen, L. A., Yokoyama, A., and Ohki, M. (2001) *EMBO J.* **20,** 7184–7196
33. Katsumoto, T., Aikawa, Y., Iwama, A., Ueda, S., Ichikawa, H., Ochiya, T., and Kitabayashi, I. (2006) *Genes Dev.* **20,** 1321–1330
34. Thomas, T., Corcoran, L. M., Gugasyan, R., Dixon, M. P., Brodnicki, T., Nutt, S. L., Metcalf, D., and Voss, A. K. (2006) *Genes Dev.* **20,** 1175–1186
35. Deguchi, K., Ayton, P. M., Carapeti, M., Kutok, J. L., Snyder, C. S., Williams, I. R., Cross, N. C., Glass, C. K., Cleary, M. L., and Gilliland, D. G. (2003) *Cancer Cell* **3,** 259–271
36. Huntly, B. J., Shigematsu, H., Deguchi, K., Lee, B. H., Mizuno, S., Duclos, N., Rowan, R., Amaral, S., Curley, D., Williams, I. R., Akashi, K., and Gilliland, D. G. (2004) *Cancer Cell* **6,** 587–596
37. Kindle, K. B., Troke, P. J., Collins, H. M., Matsuda, S., Bossi, D., Bellodi, C., Kalkhoven, E., Salomoni, P., Pelicci, P. G., Minucci, S., and Heery, D. M. (2005) *Mol. Cell. Biol.* **25,** 988–1002
38. Kitabayashi, I., Yokoyama, A., Shimizu, K., and Ohki, M. (1998) *EMBO J.* **17,** 2994–3004
39. Chittenden, T., Livingston, D. M., and DeCaprio, J. A. (1993) *Mol. Cell. Biol.* **13,** 3975–3983
40. Doyon, Y., Cayrou, C., Ullah, M., Landry, A. J., Cote, V., Selleck, W., Lane, W. S., Tan, S., Yang, X. J., and Cote, J. (2006) *Mol. Cell* **21,** 51–64
41. Canman, C. E., Lim, D. S., Cimprich, K. A., Taya, Y., Tamai, K., Sakaguchi, K., Appella, E., Kastan, M. B., and Siliciano, J. D. (1998) *Science* **281,** 1677–1679
42. Lees-Miller, S. P., Sakaguchi, K., Ullrich, S. J., Appella, E., and Anderson, C. W. (1992) *Mol. Cell. Biol.* **12,** 5041–5049
43. Siliciano, J. D., Canman, C. E., Taya, Y., Sakaguchi, K., Appella, E., and Kastan, M. B. (1997) *Genes Dev.* **11,** 3471–3481
44. D'Orazi, G., Cecchinelli, B., Bruno, T., Manni, I., Higashimoto, Y., Saito, S., Gostissa, M., Coen, S., Marchetti, A., Del Sal, G., Piaggio, G., Fanciulli, M., Appella, E., and Soddu, S. (2002) *Nat. Cell Biol.* **4,** 11–19
45. Hofmann, T. G., Moller, A., Sirma, H., Zentgraf, H., Taya, Y., Droge, W., Will, H., and Schmitz, M. L. (2002) *Nat. Cell Biol.* **4,** 1–10
46. Oda, K., Arakawa, H., Tanaka, T., Matsuda, K., Tanikawa, C., Mori, T., Nishimori, H., Tamai, K., Tokino, T., Nakamura, Y., and Taya, Y. (2000) *Cell* **102,** 849–862
47. Olivier, M., Eeles, R., Hollstein, M., Khan, M. A., Harris, C. C., and Hainaut, P. (2002) *Hum. Mutat.* **19,** 607–614
48. Soussi, T., Kato, S., Levy, P. P., and Ishioka, C. (2005) *Hum. Mutat.* **25,** 6–17
49. Vassilev, L. T., Vu, B. T., Graves, B., Carvajal, D., Podlaski, F., Filipovic, Z., Kong, N., Kammlott, U., Lukacs, C., Klein, C., Fotouhi, N., and Liu, E. A. (2004) *Science* **303,** 844–848
50. Tovar, C., Rosinski, J., Filipovic, Z., Higgins, B., Kolinsky, K., Hilton, H., Zhao, X., Vu, B. T., Qing, W., Packman, K., Myklebost, O., Heimbrook, D. C., and Vassilev, L. T. (2006) *Proc. Natl. Acad. Sci. U.S.A.* **103,** 1888–1893
51. de Stanchina, E., Querido, E., Narita, M., Davuluri, R. V., Pandolfi, P. P., Ferbeyre, G., and Lowe, S. W. (2004) *Mol. Cell* **13,** 523–535
52. Grossman, S. R. (2001) *Eur. J. Biochem.* **268,** 2773–2778

MOLECULAR AND CELLULAR BIOLOGY, Dec. 2008, p. 7126–7138 Vol. 28, No. 23
0270-7306/08/$08.00+0 doi:10.1128/MCB.00897-08

PML Activates Transcription by Protecting HIPK2 and p300 from SCF^{Fbx3}-Mediated Degradation▽†

Yutaka Shima,[1] Takito Shima,[1] Tomoki Chiba,[2] Tatsuro Irimura,[3] Pier Paolo Pandolfi,[4] and Issay Kitabayashi[1]*

Molecular Oncology Division, National Cancer Center Research Institute, 5-1-1 Tsukiji, Chuo-ku, Tokyo 104-0045, Japan[1]; Graduate School of Life and Environmental Sciences, University of Tsukuba, 1-1-1 Ten-noudai, Tsukuba, Ibaraki 305-8572, Japan[2]; Graduate School of Pharmaceutical Sciences, University of Tokyo, 7-3-1 Hongo, Bunkyo-ku, Tokyo 113-0033, Japan[3]; and Beth Israel Deaconess Medical Center and Harvard Medical School, 77 Avenue Louis Pasteur, Boston, Massachusetts 02115[4]

Received 5 June 2008/Returned for modification 7 July 2008/Accepted 12 September 2008

PML, a nuclear protein, interacts with several transcription factors and their coactivators, such as HIPK2 and p300, resulting in the activation of transcription. Although PML is thought to achieve transcription activation by stabilizing the transcription factor complex, little is known about the underlying molecular mechanism. To clarify the role of PML in transcription regulation, we purified the PML complex and identified Fbxo3 (Fbx3), Skp1, and Cullin1 as novel components of this complex. Fbx3 formed SCF^{Fbx3} ubiquitin ligase and promoted the degradation of HIPK2 and p300 by the ubiquitin-proteasome pathway. PML inhibited this degradation through a mechanism that unexpectedly did not involve inhibition of the ubiquitination of HIPK2. PML, Fbx3, and HIPK2 synergistically activated p53-induced transcription. Our findings suggest that PML stabilizes the transcription factor complex by protecting HIPK2 and p300 from SCF^{Fbx3}-induced degradation until transcription is completed. In contrast, the leukemia-associated fusion PML-RARα induced the degradation of HIPK2. We discuss the roles of PML and PML-retinoic acid receptor α, as well as those of HIPK2 and p300 ubiquitination, in transcriptional regulation and leukemogenesis.

In human leukemia, specific chromosomal translocations result in the expression of specific fusion proteins and malignancy (16, 39). The *PML* gene is the target of the t(15;17) chromosome translocation in acute promyelocytic leukemia (APL) and is fused to the retinoic acid receptor α (RARα) gene, which leads to the generation of a PML-RARα fusion protein (11, 12, 18, 28). The PML protein is known to localize in discrete nuclear speckles called PML nuclear bodies (NBs) (58). In the NBs, PML interacts with several transcription factors such as p53 and AML1, transcription coactivators such as HIPK2 and p300, and apoptosis modulators such as pRB and DAXX (27, 52, 53). PML enhances p53-dependent apoptosis by inducing p53 target genes (15, 20). Additionally, PML can lead to cell senescence by activating p53 (46). We have reported that PML interacts with AML1, a target of several chromosome translocations in leukemia (41), and stimulates the AML1-dependent differentiation of murine myeloid progenitor cells (44). APL-derived PML-RARα is thought to be dominant negative to PML. PML-RARα disrupts NBs into microspeckles (14) and inhibits DNA damage-induced apoptosis (56) and PML IV enhancement of PU.1-induced myeloid differentiation (57). Thus, PML activates and PML-RARα represses transcription. However, little is known about how PML activates transcription. Moreover, it remains unclear why transcription factors and coactivators are localized in NBs.

The ubiquitin-proteasome pathway involves two successive steps: labeling of the substrates with multiple ubiquitin molecules and degradation of the labeled substrates at the 26S proteasome. Ubiquitin conjugation is catalyzed by three enzymes: the ubiquitin-activating enzyme E1, the ubiquitin-conjugating enzyme E2, and the ubiquitin-protein ligase E3 (17). E3 ubiquitin ligases are classified into several types, including HECT-type E3, RING finger motif-containing E3, and U-box domain containing E3. MDM2, the APC/C complex, and the SCF complex are known to be the RING finger motif-containing E3 (21, 33, 54). The SCF complex is composed of F-box protein, Skp1, Cullin1 (Cul1), and ROC1. In the SCF complex, F-box proteins recognize specific substrates for ubiquitination. Therefore, the different SCF complexes are designated according to their F-box proteins (7, 24, 30). Proteins ubiquitinated by the SCF complex are degraded rapidly by the proteasome.

In this study, we purified the PML complex to clarify the role of PML in transcription and identified Fbxo3 (Fbx3), Skp1, and Cul1 as components of the PML complex. We found that Fbx3, whose substrates were unknown, formed SCF^{Fbx3} ubiquitin ligase and regulated the degradation of HIPK2 and p300 by the ubiquitin-proteasome pathway. This degradation was inhibited by PML through a mechanism that did not involve the inhibition of ubiquitination. PML, HIPK2, and Fbx3 increased p53 transcriptional activity synergistically. Our data suggest that the interplay between SCF^{Fbx3}-induced ubiquitination and degradation of transcription coactivators, such as HIPK2 and p300, and the stabilization of these coactivators by PML play critical roles in transcriptional regulation.

* Corresponding author. Mailing address: Molecular Oncology Division, National Cancer Center Research Institute, 5-1-1 Tsukiji, Chuo-ku, Tokyo 104-0045, Japan. Phone: 81 3 3547 5274. Fax: 81 3 3542 0688. E-mail: ikitabay@ncc.go.jp.

† Supplemental material for this article may be found at http://mcb.asm.org/.

▽ Published ahead of print on 22 September 2008.

MATERIALS AND METHODS

Cell culture, infection, and antibodies. K562 cells, MOLT-4 cells, H1299 cells, MCF7 cells, and NB4 cells were cultured in RPMI 1640 medium supplemented with 10% fetal calf serum (FCS). SKNO-1 cells were cultured in GIT (Wako). BOSC23 cells and PLAT-E cells were cultured in Dulbecco's modified Eagle's medium supplemented with 10% FCS. NIH 3T3 cells were cultured in Dulbecco's modified Eagle's medium supplemented with 10% calf serum. Mouse bone marrow (BM) cell suspensions were prepared by flushing isolated femora with phosphate-buffered saline (PBS), and the cells were cultured in StemPro-34 supplemented with 2.5% nutrient supplement, 2 mM L-glutamine, 10 ng/ml interleukin-3, 50 ng/ml SCF, 10 ng/ml oncostatin M, 20 ng/ml interleukin-6, 1% penicillin-streptomycin, and 0.1% tylosin. For the production of retroviruses, PLAT-E cells were transfected with pMSCV-derived retroviruses by the calcium phosphate precipitation method, and culture supernatants were collected 48 h after transfection. NIH 3T3 cells were infected by incubation in the culture supernatant of PLAT-E cells transfectants for 24 h.

Anti-HIPK2 antibody was described previously (26). Anti-Fbx3 antibody was generated by immunizing mice with glutathione *S*-transferase-tagged Fbx3. Other antibodies were purchased commercially and were as follows: antihemagglutinin (anti-HA) (3F10; Roche), anti-FLAG (M2; Sigma), anti-Gal4 (RK5C1; Santa Cruz), anti-p300 (N15; Santa Cruz), antitubulin (H235; Santa Cruz), antiubiquitin (FK2; Nippon Bio-Test), and anti-PML (001 [MBL], H238 [Santa Cruz], or 36.1-104 [UBI]).

Plasmids. Human Fbx3 cDNA was amplified by PCR from a human cDNA library generated from poly(A)$^+$ RNA of K562 cells by use of the oligonucleotides 5′-ACCGGGCCAGGCAAGATGGC-3′ as the upstream primer and 5′-GCAAACCCAAACAATCCAATTCC-3′ as the downstream primer. The N-terminal FLAG tag and HA tag were fused to Fbx3 cDNAs by use of the oligonucleotide 5′-ACGTACCGCGGACCATGGCAGACTACAAGGACGACGATGACAAGGCGGCCATGGAGACCGAGAC-3′ or 5′-ACGTACCGCGGACCATGGCATACCCATACGACGTGCCTGACTACGCTGCGGCCATGGAGACCGAGAC-3′ as the upstream primer and 5′-TCTGCGCTTCCACAGCATCG-3′ as the downstream primer in the PCR. Fbx3 deletion mutants were generated by PCR using pcDNA-HA-Fbx3 or pcDNA-FLAG-Fbx3 as the template. The PML, AML1, p300, and HIPK2 expression vectors were generated as described previously (1, 32, 37, 44, 57). p53 expression vectors and the MDM2-luc reporter were kindly provided by Y. Taya.

Purification of the PML complex. K562 cells were transfected with pLNCX or pLNCX-FLAG-PML I by electroporation. Cells stably expressing FLAG-PML I protein were cloned. The cells (~1×10^{10} cells) were lysed by sonication at 4°C in 500 ml of 500 mM NaCl lysis buffer (20 mM sodium phosphate, pH 7.0, 500 mM NaCl, 30 mM sodium pyrophosphate, 0.1% NP-40, 5 mM EDTA, 10 mM NaF, 5 mM dithiothreitol [DTT], and 1 mM phenylmethylsulfonyl fluoride [PMSF]) supplemented with Complete (Roche). The lysates were cleared by centrifugation at 40,000 × *g* for 30 min at 4°C and incubated with 2.5 ml of anti-FLAG monoclonal antibody (M2)-conjugated beads with rotation at 4°C for 12 h. The beads with absorbed PML I immunocomplexes were washed six times with 50 ml of lysis buffer (20 mM sodium phosphate, pH 7.0, 250 mM NaCl, 30 mM sodium pyrophosphate, 0.1% NP-40, 5 mM EDTA, 10 mM NaF, 5 mM DTT, and 1 mM PMSF). The PML I complexes were selectively eluted by incubating twice with 0.2 mg/ml FLAG peptide in 7.5 ml of lysis buffer for 2 h. The eluates were concentrated using a filtration device and separated by sodium dodecyl sulfate-polyacrylamide gel electrophoresis (SDS-PAGE). Proteins were stained with Coomassie brilliant blue, excised, destained with 25 mM ammonium bicarbonate and 50% acetonitrile, dried, digested with sequence-grade modified trypsin in 50 mM Tris-HCl (pH 7.6), extracted with 5% trifluoroacetic acid-50% acetonitrile, and subjected to liquid chromatography-tandem mass spectrometry analysis.

Immunoprecipitation and Western blotting. BOSC23 cells were transfected with the desired vectors. After 15 h, culture supernatants were exchanged for fresh media and cells were treated with or without 10 μM MG132 (Calbiochem) for 9 h. The cells were lysed by incubation at 4°C for 30 min in lysis buffer. The lysates were cleared by centrifugation at 40,000 × *g* for 30 min at 4°C and the supernatants were incubated with anti-FLAG antibody-conjugated beads with rotation at 4°C for 12 h. The beads were washed six times with 1 ml of lysis buffer. After being washed, the cell extracts were selectively eluted by incubating with 0.2 mg/ml FLAG peptide for 2 h.

Cell lysates and immunoprecipitates were fractionated on SDS-polyacrylamide gels and transferred onto nitrocellulose membranes (Amersham). The membranes were incubated with primary antibodies and with horseradish peroxidase-conjugated secondary antibodies. The immune complexes were visualized by the ECL or ECL-Plus technique (Amersham).

RNA interference, RT-PCR, and real-time PCR. Fbx3-specific and control small interfering RNAs (siRNAs) were purchased from Ambion. RARα-specific and control stealth siRNAs were purchased from Invitrogen. MOLT-4 cells and NB4 cells were transfected with these siRNAs by using Nucleofector (Amaxa). NIH 3T3 cells were transfected five times with these siRNAs by use of Lipofectamine 2000. For reverse transcriptase PCR (RT-PCR), total RNA was purified using an RNeasy mini kit (Qiagen), and cDNAs were transcribed using SuperScript II RT (Invitrogen). PCRs were performed using the following primers: Fbx3 (human) forward (5′-GGTGTCCTCGGATGGTTTTATCTC-3′) and reverse (5′-TCTCTGATGATGGGGAAGCCAC-3′), Fbx3 (mouse) forward (5′-ACCCTCTGCTGCTCATCTTATCC-3′) and reverse (5′-CCACTAACTTTTGCCCGTTGTG-3′), HIPK2 forward (5′-GCTTCCAGCACAAGAACCACAC-3′) and reverse (5′-GCAATGACACAACCAAGGGACC-3′), p300 forward (5′-GCAATGGACAAAAAGGCAGTTC-3′) and reverse (5′-TGAGAGGAAGACACACAGGACAATC-3′), glyceraldehyde-3-phosphate dehydrogenase forward (5′-CTTCACCACCATGGAGAAGGC-3′) and reverse (5′-GGCATGGACTGTGGTCATGAG-3′), PML-RARα forward (5′-CCAATACAACGACAGCCCAGAAG-3′) and reverse (5′-CCATAGTGGTAGCCTGAGGACTTG-3′), and RARα forward (5′-CAGAACTGCTTGACCAAAGGACC-3′) and reverse (5′-AAGGCTTGTAGATGCGGGGTAGAG-3′). Real-time PCR was performed using the 7500 fast real-time PCR system (Applied Biosystems). The expression of the *p21* gene was normalized with respect to the expression of the *TBP* gene.

In vivo degradation assay. BOSC23 cells were transfected with the desired vectors, increasing amounts of pcDNA-HA-Fbx3, and pFA-CMV for expression of the Gal4 DNA-binding domain (Gal4 BD) as an internal control. After 24 h, the cells were lysed. The lysates were analyzed by Western blotting.

In vivo ubiquitination assay. BOSC23 cells were transfected with the desired vectors. Cells were treated with 50 μM MG132 1 h before harvesting and lysed in lysis buffer. To assay the stabilization of ubiquitinated HIPK2, cells were lysed in radioimmunoprecipitation assay buffer (20 mM Tris-HCl, pH 7.5, 150 mM NaCl, 2 mM EDTA, 0.25% SDS, 1% NP-40, 1% sodium deoxycholic acid, 5 mM DTT, and 1 mM PMSF) supplemented with Complete. The lysates were incubated with anti-FLAG antibody-conjugated beads as described above. Ubiquitinated HIPK2 was detected by immunoblotting with the antiubiquitin antibody, followed by treatment with horseradish peroxidase-conjugated secondary antibodies as described above.

Immunofluorescence. MCF7 cells were cultured in four-well chamber slides and transfected with pLNCX-FLAG-PML I and pcDNA-HA-Cul1, pcDNA-HA-Fbx3, or pcDNA-HA-Skp1, or pLNCX-FLAG-PML IV and pLNCX-HA-HIPK2 or pLNCX-HA-p300 by use of Lipofectamine 2000. The cells were treated with or without 10 μM MG132 for 18 h (HIPK2) or 9 h (p300). After MG132 treatment, the cells were fixed with 4% formaldehyde in PBS and incubated with 0.2% Triton X-100 in PBS for 5 min at room temperature. Antibodies were diluted in blocking buffer (1% FCS in PBS). Cells were incubated with the primary antibodies for 12 h at 4°C and then incubated with the secondary antibodies. The slides were mounted in Vectashield (Vector Laboratories). Images were captured on an Olympus microscope.

Luciferase assay. H1299 cells were transfected using the calcium phosphate precipitation method or Lipofectamine 2000 in 24-well plates, and luciferase activity was assayed after 24 h with a Veritas luminometer (Turner Biosystems) according to the manufacturer's protocol (Promega). Results of reporter assays are represented as the mean values for relative luciferase activity generated from four independent experiments and normalized against the activity of the enzyme form phRG-TK as an internal control.

RESULTS

PML complex contains Cul1, Fbx3, and Skp1. In order to clarify the role of PML in transcription, we purified the PML complex from the cell lysates of K562 cells expressing FLAG-tagged PML I and resolved the complex by SDS-PAGE. Liquid chromatography-tandem mass spectrometry analysis identified Cul1, Fbx3, and Skp1 as components of the PML complex (Fig. 1A and B). Other proteins identified in the PML complex are shown in Table S1 in the supplemental material. To test whether Cul1, Fbx3, or Skp1 interacts with PML I, we used immunofluorescence analysis. HA-tagged Cul1, HA-tagged Fbx3, or HA-tagged Skp1 was cotransfected with FLAG-tagged PML I into MCF7 cells, and the locations of these

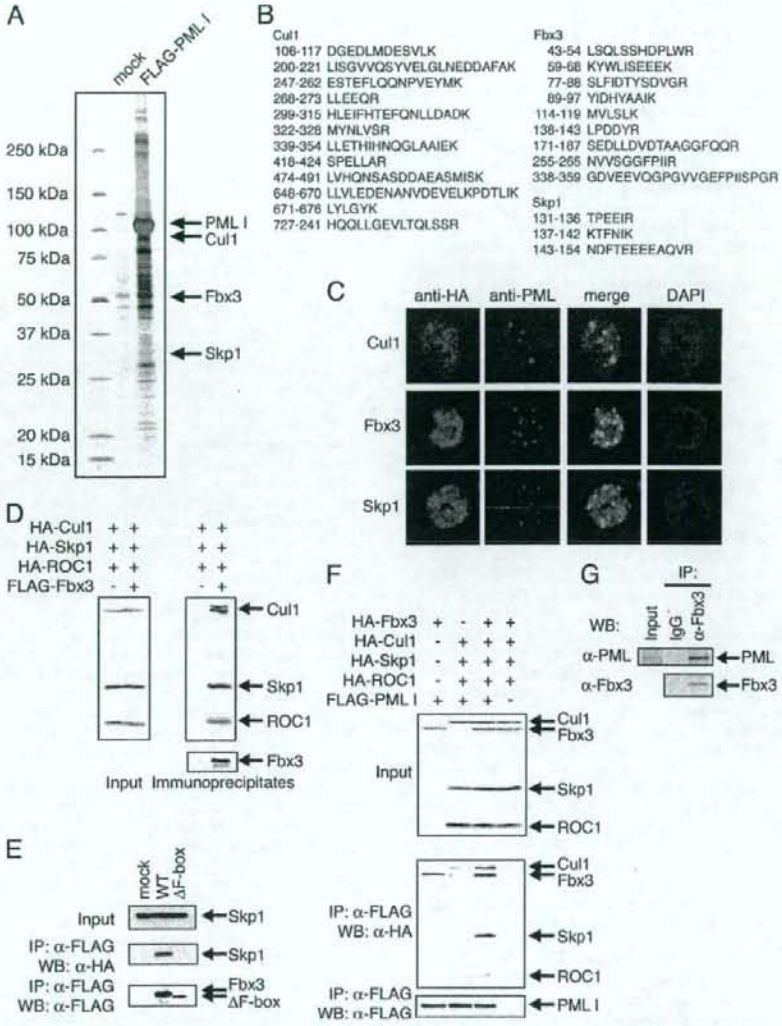

FIG. 1. Ubiquitin ligase SCF^{Fbx3} is part of the PML complex. (A) Purification of the PML complex. The PML complex was purified from cell lysates prepared from K562 cells carrying an empty vector (mock) or stably expressing FLAG-tagged PML I. The complexes were incubated with anti-FLAG antibody-conjugated agarose, and the bound materials were eluted with the FLAG peptide. The eluates were resolved by SDS-PAGE and visualized by silver staining. The proteins were identified by mass spectrometry. (B) The amino acid sequences of the peptides derived from the fractions specific to the FLAG-PML I-expressing cells. The proteins in the specific fractions were identified as Cul1, Fbx3, and Skp1. (C) Cul1, Fbx3, and Skp1 colocalized with PML I. MCF7 cells were cotransfected with pLNCX-FLAG-PML I and pcDNA-HA-Cul1, pcDNA-HA-Fbx3, or pcDNA-HA-Skp1. Cul1, Fbx3, and Skp1 were stained with anti-HA antibody and PML I was stained with anti-PML (001) antibody. DAPI, 4′,6′-diamidino-2-phenylindole. (D) Fbx3 forms a complex with Skp1, Cul1, and ROC1. BOSC23 cells were transfected with pcDNA-HA-Skp1, pcDNA-HA-Cul1, pcDNA-HA-ROC1, and either the empty vector (−) or pcDNA-FLAG-Fbx3. The expression of Skp1, Cul1, and ROC1 in the lysates of transfectants was detected by immunoblotting using anti-HA antibody (left). The Fbx3 complex was immunoprecipitated with anti-FLAG antibody. The immunoprecipitates were analyzed by immunoblotting using anti-HA and anti-FLAG antibodies (right). (E) The F-box domain is required for the interaction between Fbx3 and Skp1. BOSC23 cells were transfected with pcDNA-HA-Skp1 and either mock or pcDNA-FLAG-Fbx3 constructs as indicated. The expression of Skp1 in the lysates of transfectants was detected by immunoblotting using anti-HA antibody (top). The lysates of transfectants were incubated with anti-FLAG antibody. The immunoprecipitates were analyzed by immunoblotting using anti-HA (middle) and anti-FLAG (bottom) antibodies. (F) PML interacts with SCF^{Fbx3} through Fbx3. BOSC23 cells were cotransfected with pcDNA-HA-Fbx3, pcDNA-HA-Skp1, pcDNA-HA-Cul1, pcDNA-HA-ROC1, and either mock empty vector or pLNCX-FLAG-PML I. The interactions between PML I and components of SCF^{Fbx3} were analyzed as described for panel D. (G) Endogenous Fbx3 interacts with endogenous PML. SKNO-1 cells were lysed and Fbx3 was immunoprecipitated with anti-Fbx3 antibody. The immunoprecipitates were analyzed by immunoblotting with anti-Fbx3 and anti-PML (H238) antibodies. IP, immunoprecipitate; WB, Western blot; α-, anti-.

proteins were detected by anti-HA antibody (Cul1, Fbx3, or Skp1) or anti-PML antibody (PML I). PML I was localized in NBs, and Cul1, Fbx3, or Skp1 was colocalized with PML I at the peripheries of NBs (Fig. 1C). Colocalization of Fbx3 with PML I was detected more significantly than that of Cul1 and Skp1 (Fig. 1C). Cul1 and Skp1 are known to be components of SCF ubiquitin ligase (17). The function of Fbx3 was unknown, but it contains the F-box domain, which is found in a component of the SCF complex that determines substrate specificity (24). To confirm that Fbx3 was a component of the SCF complex, BOSC23 cells were transfected with FLAG-tagged Fbx3 and HA-tagged Skp1, Cul1, and ROC1. In immunoblot analysis, HA-tagged Skp1, Cul1, and ROC1 coprecipitated with FLAG-tagged Fbx3 (Fig. 1D). The F-box domain is known to be a Skp1 interaction site (30). Therefore, we examined whether the F-box domain of Fbx3 was required for interaction with Skp1. The Fbx3 mutant lacking the F-box domain (ΔF-box mutant; deletion of the region from 61 to 471) did not coprecipitate with Skp1 (Fig. 1E). These results suggest that Fbx3 can form an SCF ubiquitin ligase (SCF^{Fbx3}).

As shown in Fig. 1A, components of SCF^{Fbx3} were present in the PML complex. A coimmunoprecipitation assay was performed to determine the component of SCF^{Fbx3} that was primarily responsible for mediating its interaction with PML. When cotransfected together, all of the components of SCF^{Fbx3}, including Fbx3, Skp1, Cul1, and ROC1, were efficiently coprecipitated with PML (Fig. 1F). However, PML could not be coprecipitated with Skp1, Cul1, or ROC1 efficiently without cotransfection with Fbx3 (Fig. 1F). In addition, a strong interaction between PML and Fbx3 was detected without cotransfection of the other SCF^{Fbx3} components. To assess whether endogenous PML interacted with endogenous Fbx3, we performed coimmunoprecipitation assays. We found that endogenous PML was efficiently coprecipitated with endogenous Fbx3 (Fig. 1G). These results suggest that Fbx3 mediates the interaction between SCF^{Fbx3} and PML.

Since several isoforms of PML are known, we tested the interactions between PML isoforms and Fbx3. Coimmunoprecipitation analysis indicated that Fbx3 could be coprecipitated with all PML isoforms tested (I to VI) (Fig. 2A). To determine the domains in Fbx3 that are required for interaction with PML, HA-tagged PML I was cotransfected with FLAG-tagged Fbx3 deletion mutants, as shown schematically in Fig. 2B. Deletion of the regions from 341 to 404 and from 1 to 60 of Fbx3 are required for interaction with PML (Fig. 2C). The Fbx3 mutant (deletion of 61 to 340), which does not contain both regions, did not interact with PML I at all. To determine the domains in PML that are required for the interaction with Fbx3, FLAG-tagged Fbx3 was cotransfected with HA-tagged wild-type or truncated versions of PML, as shown schematically in Fig. 2D. Removal of the N-terminal proline-rich (Pro) region (1 to 55), the coiled-coil region (217 to 329), or the serine-proline region (502 to 553) did not affect the interaction with Fbx3. C-terminal deletions up to amino acid 343 did not affect the interaction, but further deletion up to 313 resulted in the loss of interaction (Fig. 2E). However, Fbx3 interacted with the PML mutant truncated between amino acids 330 and 342 (Fig. 2F). Fbx3 also interacted with the PML mutant with a truncation in its N-terminal region (Fig. 2F). Thus, the Fbx3 interaction sites of PML are located between amino acids 330 and 342, close to the coiled-coil region, and in the C-terminal region.

Fbx3 stimulates PML-mediated transcriptional activity of p53. PML is known to activate p53-dependent transcription (15, 20). The fact that Fbx3 is a part of the PML complex (Fig. 1A) suggested that Fbx3 functions in PML-dependent transcriptional activation. To test the effect of Fbx3 on p53-dependent transcription, we performed reporter analyses using the MDM2 promoter. As shown in Fig. 3A, lane 8, PML IV activated p53-dependent transcription, as previously reported (15, 20). Although Fbx3 alone had little effect on p53-dependent transcription (Fig. 3A, lane 9), it activated p53-dependent transcription when cotransfected with PML IV (Fig. 3A, lane 11). In contrast, the ΔF-box mutant, which cannot form the SCF complex, did not activate transcription even in the presence of PML IV (Fig. 3A, lane 12). As shown in Fig. 2E, the region from amino acid 330 to 342 and the C-terminal region of PML are important for its interaction with Fbx3. We examined whether PML mutants lacking these regions (PML IV Δ330-342 and Δ502-882) would activate p53-dependent transcription. Unlike the PML IV wild type, PML IV Δ330-342 and Δ502-882 did not activate p53-mediated transcription (Fig. 3B). To determine whether Fbx3 is involved in PML-dependent transcriptional activation, we performed reporter analyses using siRNAs for Fbx3. Fbx3-specific siRNA (siFbx3) inhibited PML-dependent transcriptional activation, in contrast to the control siRNA (siControl) (Fig. 3C). The induction of *p21*, a p53 target gene, is known to be impaired in $PML^{-/-}$ cells (20). To examine whether Fbx3 contributes to the expression of *p21*, we used siRNA to knock down endogenous Fbx3 expression. Fbx3 depletion by siRNA impaired the adriamycin (ADR)-induced expression of *p21* (Fig. 3D). Thus, SCF^{Fbx3} stimulates PML-dependent transcriptional activation. These results suggest that the ubiquitination substrates of SCF^{Fbx3} are factors that are involved in PML-dependent transcriptional activation.

HIPK2 and p300 are the targets of SCF^{Fbx3}. It has been reported that PML, HIPK2, and p300 activate p53-dependent transcription (3, 13, 22, 38, 42) as well as AML1-dependent transcription (1, 32, 44). p53, AML1, HIPK2, and p300 are known to interact with PML and therefore could be potential targets of SCF^{Fbx3}. To test whether Fbx3 promoted the degradation of these proteins, increasing amounts of Fbx3 were cotransfected with PML I, PML IV, p53, AML1, HIPK2, and p300. Although Fbx3 had no effect on the levels of PML I, PML IV, p53, or AML1 (Fig. 4A), it decreased the levels of HIPK2 and p300 in a dose-dependent manner (Fig. 4A). These decreases were inhibited by the proteasome inhibitor MG132 (Fig. 4A). The ΔF-box mutant did not decrease the levels of either HIPK2 or p300 (Fig. 4B). To examine whether endogenous HIPK2 and p300 were degraded by Fbx3, NIH 3T3 cells were infected with an empty retrovirus or a retrovirus encoding Fbx3 and cultured in the absence or presence of MG132. Immunoblot analysis indicated that Fbx3 overexpression decreased the levels of endogenous HIPK2 and p300 in the absence of MG132 but not in the presence of MG132 (Fig. 4C). These results suggest that SCF^{Fbx3} induces a proteasome-dependent degradation of HIPK2 and p300.

To determine whether endogenous HIPK2 and p300 were degraded by endogenous SCF^{Fbx3}, we used siRNA to knock down endogenous Fbx3 expression. Transfection of NIH 3T3

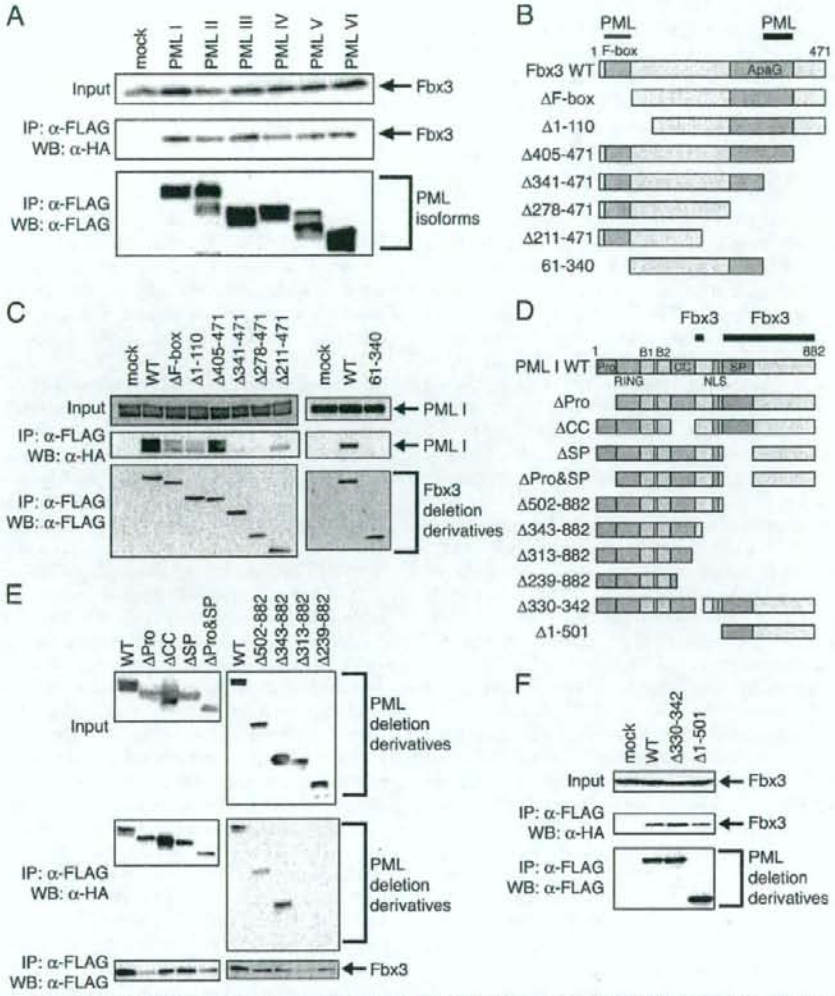

FIG. 2. PML and Fbx3 interact with their respective specific domains. (A) PML isoforms interact with Fbx3. BOSC23 cells were transfected with pLNCX-HA-Fbx3 and either mock or pLNCX-FLAG-PML isoforms (I to VI). The expression of Fbx3 in the lysates of transfectants was detected by immunoblotting using anti-HA antibody (top). The lysates of transfectants were incubated with anti-FLAG antibody. The immunoprecipitates were analyzed by immunoblotting using anti-HA (middle) and anti-FLAG (bottom) antibodies. (B) Schematic diagram of the structures of Fbx3 deletion mutants. PML indicates the strongly interacting (thick line) and weakly interacting (thin line) regions of Fbx3 as determined for panel C. (C) Identification of Fbx3 regions required for interaction with PML. BOSC23 cells were transfected with pLNCX-HA-PML I and mock or pcDNA-FLAG-Fbx3 deletion constructs as indicated. The expression of PML I in the lysates of transfectants was detected by immunoblotting using anti-HA antibody (top). The lysates of transfectants were incubated with anti-FLAG antibody. The immunoprecipitates were analyzed by immunoblotting using anti-HA (middle) and anti-FLAG (bottom) antibodies. (D) Schematic diagram of the structures of PML deletion mutants. The proline-rich region (Pro), the RING finger domain (RING), B-box domain 1 (B1), B-box domain 2 (B2), the coiled-coil domain (CC), the nuclear import signal (NLS), and the serine-proline-rich region (SP) are indicated. Fbx3 indicates the interacting region of PML as determined for panels E and F. (E and F) Identification of PML regions required for interaction with Fbx3. BOSC23 cells were cotransfected with pLNCX-FLAG-Fbx3 and pLNCX-HA-PML deletion constructs (E) or with pcDNA-HA-Fbx3 and pLNCX-FLAG-PML deletion constructs (F) as indicated. The interactions between Fbx3 and the PML mutants were analyzed as described for panel C. IP, immunoprecipitate; WB, Western blot; WT, wild type; α-, anti-.

cells with Fbx3 siRNA resulted in a decrease in Fbx3 mRNA levels (Fig. 4D, top). Fbx3 depletion by siRNA did not affect HIPK2 and p300 mRNA levels (Fig. 4D, top) but rather increased HIPK2 and p300 protein levels (Fig. 4D, bottom). These data demonstrate that the stability of HIPK2 and p300 is regulated by SCF^{Fbx3}.

In order to clarify whether SCF^{Fbx3} degrades HIPK2 by the ubiquitin-proteasome pathway, we examined whether Fbx3 in-

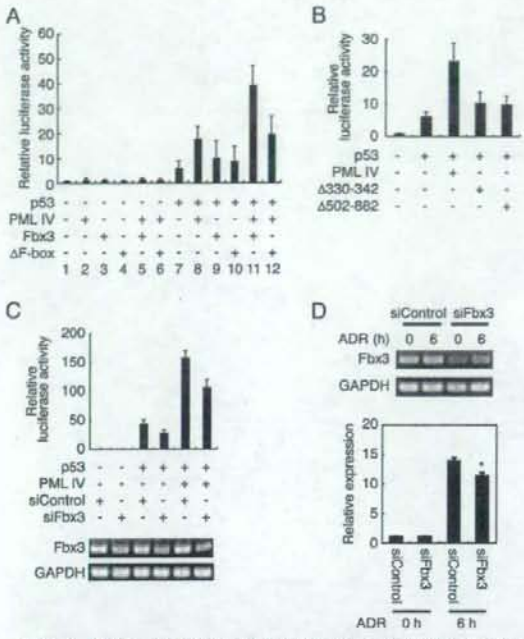

FIG. 3. PML and Fbx3 cooperatively activate p53-mediated transcription. (A) Fbx3 activates p53-mediated transcription cooperatively with PML. H1299 cells were cotransfected with 200 ng of MDM2-luc, 50 ng of phRG-TK, and 5 ng of pLNCX-FLAG-p53, 100 ng of pLNCX-HA-PML IV, and/or 200 ng of pcDNA-HA-Fbx3 or pcDNA-HA-ΔF-box. Cell lysates were analyzed for luciferase activity at 24 h after transfection. Values represent means ± standard errors of the means (SEM) from four independent determinations. (B) The Fbx3 interaction sites of PML are needed for the activation of p53-dependent transcription. H1299 cells were cotransfected with 200 ng of MDM2-luc, 50 ng of phRG-TK, and 5 ng of pLNCX-FLAG-p53 and/or 100 ng of pLNCX-FLAG-PML IV, pLNCX-FLAG-PML IV Δ330-342, or pLNCX-HA-PML Δ502-882. Cell lysates were analyzed for luciferase activity at 24 h after transfection. Values represent means ± SEM from four independent determinations. (C) Fbx3 is involved in PML-dependent transcriptional activation. H1299 cells were cotransfected with 200 ng of MDM2-luc, 50 ng of phRG-TK, 5 ng of pLNCX-FLAG-p53, and 50 ng of pLNCX-FLAG-PML IV and/or 100 pmol siControl or siFbx3 by using Lipofectamine 2000. Cell lysates were analyzed for luciferase activity at 24 h after transfection. Values represent means ± SEM from four independent determinations (top). The primers for RT-PCR (bottom) are described in Materials and Methods. (D) Expression of *p21* is decreased by knocking down Fbx3. MOLT-4 cells were transfected with siControl or siFbx3 and then treated with 0.5 μM ADR. The primers for RT-PCR (top) are described in Materials and Methods. The expression of *p21* was analyzed by real-time PCR (bottom). Values represent means ± SEM from four independent determinations. *, *P* value of <0.001 compared with the siControl value for the 6-h time point. GAPDH, glyceraldehyde-3-phosphate dehydrogenase.

duced the ubiquitination of HIPK2. BOSC23 cells were transfected with FLAG-tagged HIPK2 and HA-tagged Fbx3 and then treated with MG132. HIPK2 proteins were immunoprecipitated with anti-FLAG antibody. Western blot analysis of the immunoprecipitates by use of antiubiquitin antibody indicated that Fbx3 stimulated the ubiquitination of HIPK2 (Fig. 4E). However, the ΔF-box mutant did not stimulate the ubiquitination of HIPK2 (see Fig. S1 in the supplemental material). These results suggest that SCF^{Fbx3} induces the ubiquitination of HIPK2. Unfortunately, we could not detect the ubiquitination of p300. This may have been because the large size of polyubiquitinated p300 prevented its efficient transfer to filters during immunoblotting.

In general, an F-box protein in the SCF complex interacts with the target proteins (30). To confirm that HIPK2 and p300 are the targets of SCF^{Fbx3}, we examined whether Fbx3 interacts with HIPK2 and p300. BOSC23 cells were transfected with HA-tagged Fbx3 and FLAG-tagged HIPK2 or p300. Fbx3 coprecipitated with HIPK2 or p300 only when MG132 was added (Fig. 4F), most likely because HIPK2 and p300 interaction with Fbx3 resulted in their immediate degradation by the proteasome. HIPK2 interacted with the N-terminal and C-terminal regions of Fbx3 (see Fig. S2 in the supplemental material). In contrast, PML, which is not a substrate for SCF^{Fbx3}, interacted equally with Fbx3 in the presence or absence of MG132 (Fig. 4G).

PML inhibits Fbx3-induced degradation of HIPK2 and p300. The fact that SCF^{Fbx3} is a part of the PML complex (Fig. 1A) suggested that PML plays a role in the Fbx3-mediated degradation of HIPK2 and p300 by the ubiquitin-proteasome pathway. To test this possibility, BOSC23 cells were transfected with FLAG-tagged HIPK2 or p300, HA-tagged Fbx3, and HA-tagged PML IV. Western blot analysis showed that PML IV inhibited the Fbx3-mediated degradation of HIPK2 and p300 (Fig. 5A and B). We examined whether PML mutants lacking the Fbx3-interacting regions (PML IV Δ330-342 and Δ502-882) would inhibit the Fbx3-mediated degradation of HIPK2. PML IV Δ330-342 did not inhibit the Fbx3-mediated degradation of HIPK2 (see Fig. S3A in the supplemental material). However, PML IV Δ502-882 inhibited the Fbx3-mediated degradation of HIPK2 (data not shown). These results indicate that the region of amino acids 330 to 342 of PML is important for the stabilization of HIPK2. To examine the effect of PML on the stability of endogenous p300, BM cells from wild-type and *Pml*$^{-/-}$ mice were treated with cycloheximide (CHX), an inhibitor of protein synthesis. After CHX treatment, endogenous p300 was degraded faster in *Pml*$^{-/-}$ cells than in wild-type cells (Fig. 5C; also see Fig. S3B in the supplemental material). Endogenous HIPK2 was not detected in wild-type or *Pml*$^{-/-}$ BM cells or in murine embryonic fibroblasts (data not shown). These data suggest that PML stabilizes p300 by inhibiting its SCF^{Fbx3}-mediated degradation.

PML is known to accumulate in NBs together with many other proteins, such as HIPK2 and p300. We hypothesized that PML might stabilize HIPK and p300 by sequestering them in NBs away from ubiquitin-proteasome-related proteins in the nucleus. We used immunofluorescence analysis to test this hypothesis. HA-tagged HIPK2 or HA-tagged p300 was cotransfected with FLAG-tagged PML IV into MCF7 cells, and the locations of these proteins were detected by anti-HA antibody and anti-PML antibody, respectively. Without cotransfection with PML, HIPK2 was localized in microspeckles and p300 showed a diffuse staining pattern in the nucleus (Fig. 5D). When coexpressed with PML IV, HIPK2 and p300 colocalized with PML IV in NBs (Fig. 5E). When HIPK2 and p300 were cotransfected with PML IV, followed by treatment with

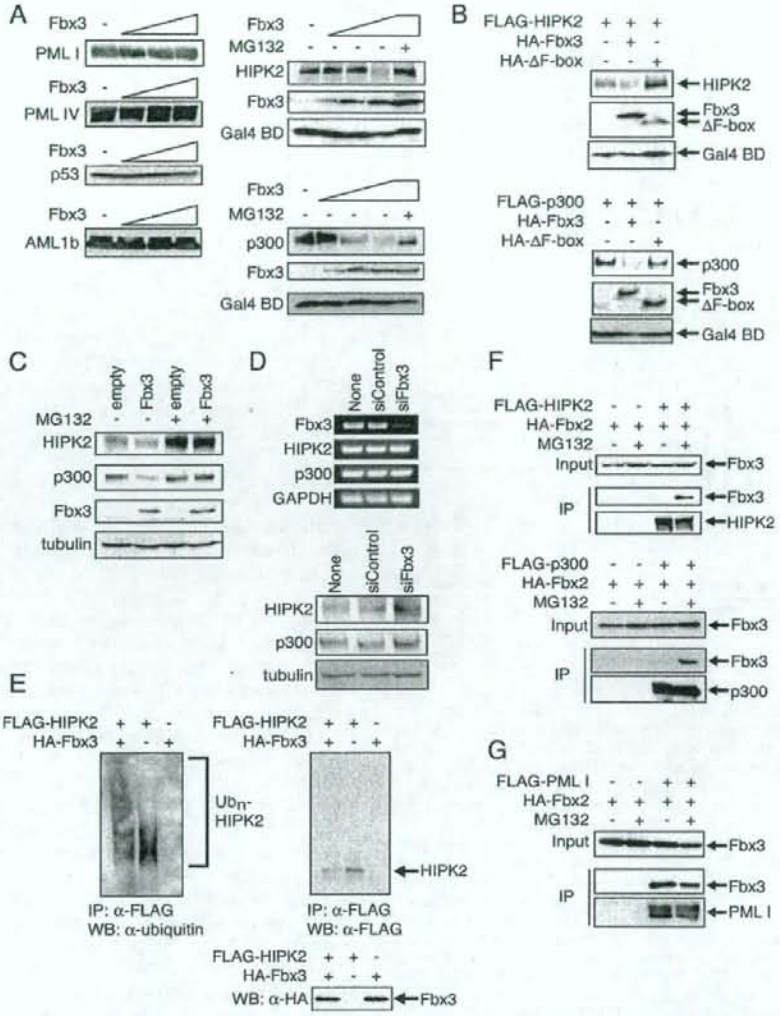

FIG. 4. HIPK2 and p300 are the targets of SCF^{Fbx3}. (A) Fbx3 induces the degradation of HIPK2 and p300. BOSC23 cells were cotransfected with 200 ng of pLNCX-FLAG-PML I, pLNCX-FLAG-PML IV, pLNCX-FLAG-p53, pLNCX-FLAG-AML1b, pLNCX-FLAG-HIPK2, or pLNCX-FLAG-p300; 100 ng of pFA-CMV for the expression of Gal4 BD as an internal control; and increasing amounts of pcDNA-HA-Fbx3 (0, 50, 200, and 800 ng). The expression of PML I, PML IV, p53, AML1, HIPK2, or p300 in the lysates of transfectants was detected by immunoblotting using anti-FLAG antibody. The expression of Fbx3 and Gal4 BD in the lysates of transfectants was detected by immunoblotting using anti-HA and anti-Gal4 antibodies, respectively. MG132 was added as described in Materials and Methods. (B) The F-box domain of Fbx3 is essential for the degradation of HIPK2 and p300. BOSC23 cells were cotransfected with pLNCX-FLAG-HIPK2 or pLNCX-FLAG-p300, pcDNA-HA-Fbx3 or pcDNA-HA-ΔF-box, and pFA-CMV. The cell lysates were analyzed as described for panel A. (C) Overexpression of Fbx3 induces the degradation of endogenous HIPK2 and p300. NIH 3T3 infectants with an empty retrovirus (empty) or a retrovirus encoding Fbx3, cultured in the absence or presence of MG132, were lysed in SDS-PAGE sample buffer. The expression of HIPK2, p300, Fbx3, and tubulin was detected by immunoblotting using anti-HIPK2, anti-p300, anti-HA, and antitubulin antibodies, respectively. (D) Expression of HIPK2 and p300 is increased by knocking down Fbx3. NIH 3T3 cells were transfected with siControl or siFbx3 five times. The primers for the RT-PCR (top) are described in Materials and Methods. The expression of HIPK2, p300, and tubulin was analyzed by Western blotting (bottom) using anti-HIPK2, anti-p300, and antitubulin, respectively. GAPDH, glyceraldehyde-3-phosphate dehydrogenase. (E) Fbx3 ubiquitinates HIPK2. BOSC23 cells were transfected with the desired vectors. Cells were treated with 50 μM MG132 and lysed. The lysates were immunoprecipitated with anti-FLAG antibody as described in Materials and Methods. The ubiquitination of HIPK2 was analyzed by immunoblotting using antiubiquitin. (F) HIPK2 and p300 interact with Fbx3 in the presence of MG132. BOSC23 cells were cotransfected with pcDNA-HA-Fbx3 and mock empty vector, pLNCX-FLAG-HIPK2 (top), or pLNCX-FLAG-p300 (bottom). Cells were treated with or without 10 μM MG132 for 9 h. The expression of Fbx3 in the lysates of transfectants was detected by immunoblotting using anti-HA antibody (Input). The lysates of transfectants were incubated with anti-FLAG antibody. The immunoprecipitates were analyzed by immunoblotting using anti-HA antibodies (middle) and anti-FLAG antibodies (bottom). (G) PML interacts with Fbx3. BOSC23 cells were transfected with pcDNA-HA-Fbx3 and either mock empty vector or pLNCX-FLAG-PML I. The interaction between Fbx3 and PML I was analyzed as described for panel F. IP, immunoprecipitate; WB, Western blot; α-, anti-.

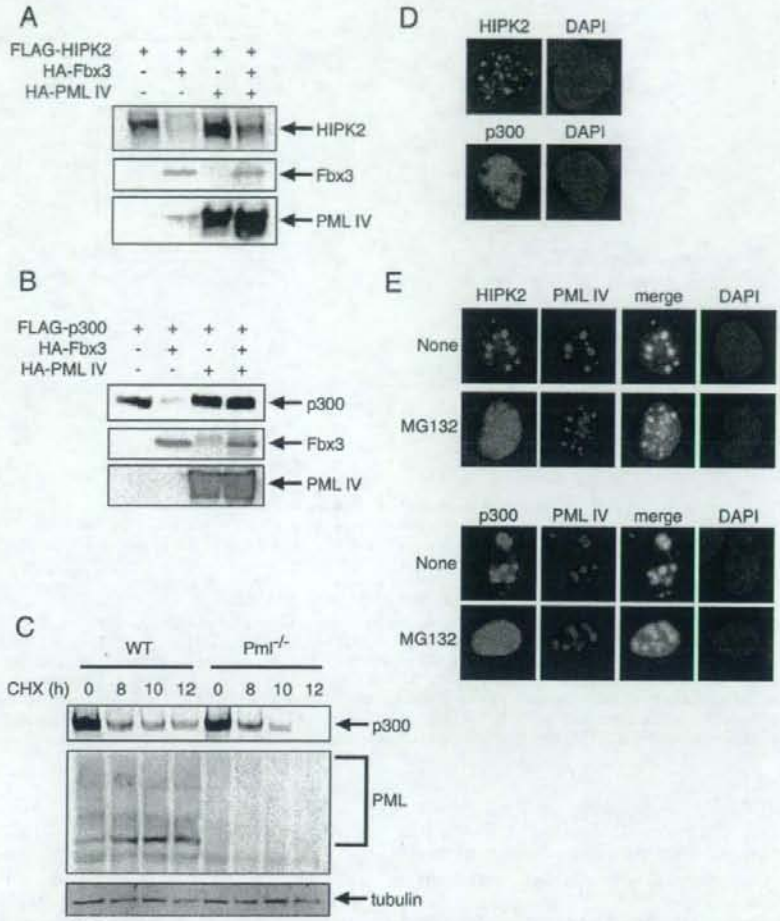

FIG. 5. PML inhibits SCF^{Fbx3}-induced degradation of HIPK2 and p300. (A) PML inhibits the degradation of HIPK2 by Fbx3. pLNCX-FLAG-HIPK2 (200 ng) and pcDNA-HA-Fbx3 (800 ng) and/or pLNCX-HA-PML IV (250 ng) were cotransfected into BOSC23 cells. The expression of HIPK2 in the lysates of transfectants was detected by immunoblotting using anti-FLAG antibody (top). The expression of Fbx3 (middle) and PML IV (bottom) in the lysates of transfectants was detected by immunoblotting using anti-HA antibody. (B) PML inhibits the degradation of p300 by Fbx3. pLNCX-FLAG-p300 (200 ng) and pcDNA-HA-Fbx3 (800 ng) and/or pLNCX-HA-PML IV (200 ng) were cotransfected into BOSC23 cells. The expression of p300 (top), Fbx3 (middle), and PML IV (bottom) was detected as described for panel A. (C) PML stabilizes p300. Wild-type (WT) and $Pml^{-/-}$ BM cells were treated with 100 μg/ml CHX. The expression of p300, PML, and tubulin was detected by immunoblotting using anti-p300, anti-PML (36.1-104), and antitubulin antibodies, respectively. (D) Localization of HIPK2 and p300 in the nucleus. MCF7 cells were transfected with pLNCX-HA-HIPK2 or pLNCX-HA-p300. The localization of HIPK2 and p300 was analyzed by use of anti-HA antibody. (E) HIPK2 and p300 are localized outside of NBs in the presence of MG132. MCF7 cells were cotransfected with pLNCX-FLAG-PML IV and pLNCX-HA-HIPK2 or pLNCX-HA-p300. Cells were treated with or without 10 μM MG132. HIPK2 and p300 were stained with anti-HA antibody and PML IV was stained with anti-PML (001) antibody. DAPI, 4′,6′-diamidino-2-phenylindole.

MG132, HIPK2 and p300 were localized to both the inside and outside of NBs. In contrast, PML was localized only in NBs before and after treatment with MG132 (Fig. 5E). Thus, MG132 stabilized HIPK2 and p300 outside of the NBs but not in the NBs. These results suggest that HIPK2 and p300 are degraded by the ubiquitin-proteasome pathway when located outside of NBs and stabilized by PML when located within NBs.

PML does not inhibit the ubiquitination of HIPK2 by SCF^{Fbx3}. PML inhibited the degradation of HIPK2 by SCF^{Fbx3} (Fig. 5A). To test whether PML affects the Fbx3-induced ubiquitination of HIPK2, BOSC23 cells were cotransfected with FLAG-tagged HIPK2, HA-tagged Fbx3, and HA-tagged PML IV. Without proteasome inhibitors, Fbx3 induced the degradation of HIPK2 (Fig. 6A, lane 3), and PML inhibited this degradation of HIPK2 (Fig. 6A, lane 4). However, the levels of

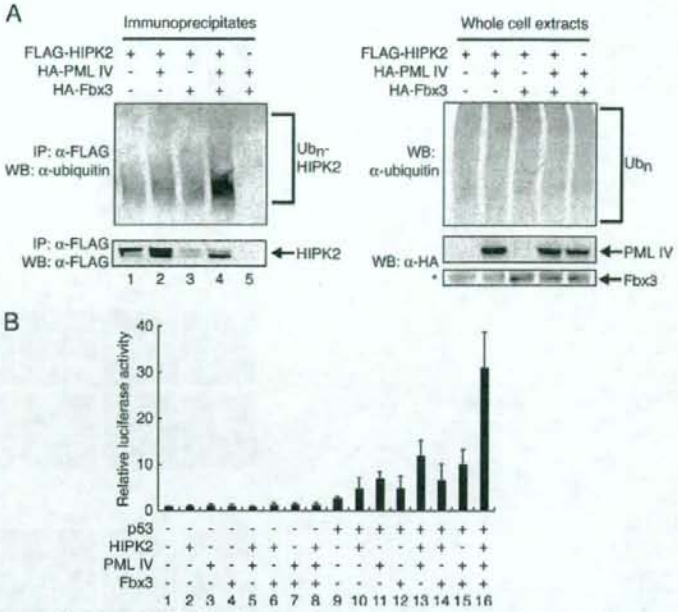

FIG. 6. PML stabilization of ubiquitinated HIPK2 is related to the transcriptional activity of p53. (A) PML stabilizes ubiquitinated HIPK2. BOSC23 cells were transfected with pLNCX-FLAG-HIPK2 and/or pcDNA-HA-Fbx3 and/or pLNCX-HA-PML IV. Cells were lysed as described in Materials and Methods. The immunoprecipitates by anti-FLAG antibody were analyzed by immunoblotting using antiubiquitin antibody. The asterisk indicates a nonspecific band present in all samples. (B) HIPK2, PML, and Fbx3 activate p53-dependent transcription synergistically. H1299 cells were cotransfected with 200 ng of MDM2-luc, 50 ng of phRG-TK, and 2.5 ng of pLNCX-FLAG-p53 or 700 ng of pLNCX-HA-HIPK2, 100 ng of pLNCX-HA-PML IV, and/or 200 ng of pcDNA-HA-Fbx3 as indicated. Cell lysates were analyzed for luciferase activity at 24 h after transfection. Values represent means ± SEM from four independent determinations. IP, immunoprecipitate; WB, Western blot; α-, anti-.

ubiquitinated HIPK2 were increased when HIPK2 was cotransfected together with both PML and Fbx3 (Fig. 6A, lane 4). These results suggest that PML inhibits the degradation of HIPK2 through a mechanism that does not involve the inhibition of its ubiquitination by SCF^{Fbx3}.

It has been reported that HIPK2 activates p53-dependent transcription (13, 22). To clarify the roles of HIPK2, PML IV, and Fbx3 in p53-dependent transcription, we performed reporter analyses using the MDM2 promoter with H1299 cells. HIPK2 increased p53 transcriptional activity (Fig. 6B, lane 10) as previously reported. Furthermore, HIPK2 and PML IV activated p53-mediated transcription cooperatively (Fig. 6B, lane 13). Since Fbx3 promotes the degradation of HIPK2, we initially thought that Fbx3 might inhibit the activation of p53-dependent transcription by HIPK2 and PML IV. However, Fbx3 stimulated this transcriptional activation (Fig. 6B, lane 16). These results are consistent with the results in Fig. 3A, which show that Fbx3 increases PML IV-mediated p53 transcriptional activity. Thus, HIPK2, PML IV, and Fbx3 activate p53-dependent transcription synergistically.

PML-RARα destabilizes HIPK2. PML-RARα is known to be a dominant-negative form of PML (49, 57). Therefore, we hypothesized that PML-RARα would not stabilize HIPK2. To test whether PML-RARα affects the stability of HIPK2, FLAG-tagged HIPK2 was mock transfected or cotransfected with PML IV or PML-RARα. As shown in Fig. 7A, the levels of HIPK2 did not decrease when it was cotransfected with PML IV. In contrast, the levels of HIPK2 decreased when it was transfected with PML-RARα. The stability of HIPK2 was also decreased by PML-RARα (Fig. 7B). This decrease in HIPK2 levels was rescued by adding MG132 (Fig. 7C and D). These data indicate that PML-RARα promotes the degradation of HIPK2 in a ubiquitin-proteasome-dependent manner. HIPK2 levels also decreased when it was cotransfected with the PML-RARα mutant truncated between amino acids 330 and 342 (see Fig. S4 in the supplemental material). To examine whether PML-RARα destabilizes endogenous HIPK2, we used siRNA for RARα to knock down PML-RARα expression in APL-derived NB4 cells. PML-RARα depletion increased the expression of endogenous HIPK2 (Fig. 7E). These results suggest that PML-RARα enhances HIPK2 degradation not by directly binding to Fbx3 but by inhibiting PML's stabilization of HIPK2.

DISCUSSION

HIPK2 and p300 are novel targets of SCF^{Fbx3}. In this study, we identified Fbx3 as a PML-interacting protein and as a subunit of SCF ubiquitin ligase that promoted the degradation of HIPK2 by the ubiquitin-proteasome pathway. Recently, Rinaldo and coworkers showed that MDM2 induced the degradation of HIPK2 in response to cytostatic doses of ADR or

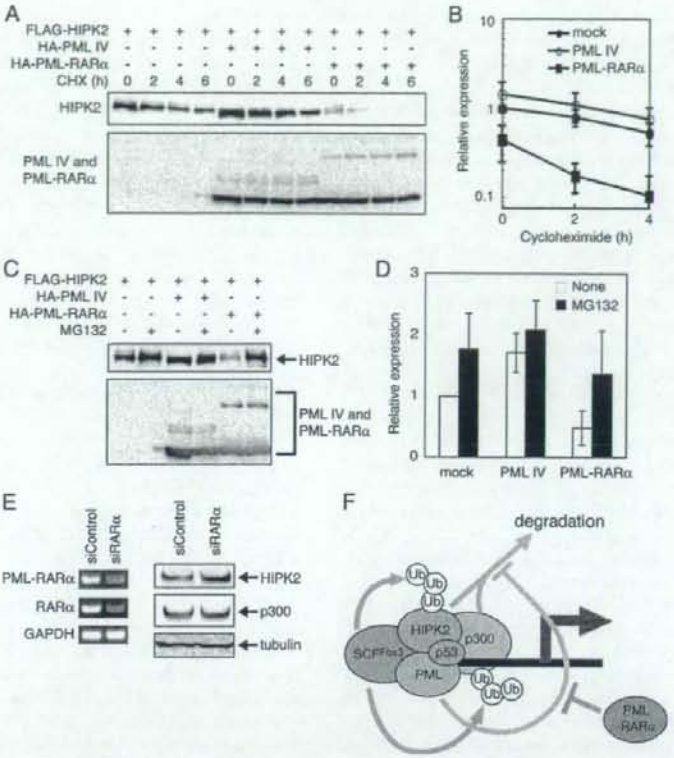

FIG. 7. PML-RARα destabilizes HIPK2. (A) PML-RARα enhances the degradation of HIPK2. BOSC23 cells were transfected with the appropriate vectors. Cells were treated with 100 μg/ml CHX and lysed. The expression of HIPK2 (top) and PML IV or PML-RARα (bottom) was detected by immunoblotting using anti-FLAG and anti-HA antibodies, respectively. (B) Quantitative analysis of HIPK2 levels following CHX treatment. Values were normalized to the mock value at the zero time point. Values represent means ± SEM from four independent determinations. (C) PML-RARα promotes the degradation of HIPK2 by the ubiquitin-proteasome pathway. BOSC23 cells were transfected with the appropriate vectors. Cells were treated with 10 μM MG132 and lysed. The lysates were analyzed as described for panel A. (D) Quantitative analysis of HIPK2 levels following MG132 treatment. Values were normalized to the nontreated mock value. Values represent means ± SEM from four independent determinations. (E) PML-RARα depletion increases the expression of HIPK2. NB4 cells were transfected with siControl or RARα-specific siRNA (siRARα). The primers for RT-PCR (left) are described in Materials and Methods. The expression of HIPK2, p300, and tubulin was analyzed by Western blot analysis (right) using anti-HIPK2, anti-p300, and antitubulin antibodies, respectively. GAPDH, glyceraldehyde-3-phosphate dehydrogenase. (F) A model for PML-mediated transcriptional activation. HIPK2 and p300 are the targets of SCF^{Fbx3}. Without PML, SCF^{Fbx3} degrades HIPK2 and p300 by the ubiquitin-proteasome pathway. PML stabilizes HIPK2 and p300 and inhibits their SCF^{Fbx3}-induced degradation. This stabilization of transcription coactivators by PML may activate transcription. PML-RARα acts as a dominant-negative inhibitor and destabilizes transcription coactivators. Ub, ubiquitin.

UV irradiation and that the C-terminal region of HIPK2 is critical for this degradation (50). Gresko and coworkers showed that the sumoylation of human HIPK2 at lysine 25 increased its stability (19). However, in this study, we found that Fbx3 could degrade mutants of HIPK2 deleted for the C-terminal region containing the lysine residue required for MDM2-mediated degradation, as well as the kinase-dead mutant (mutation of lysine 221 to alanine) and the HIPK2 K25R mutant, which cannot be sumoylated (see Fig. S5B in the supplemental material), and that Fbx3 depletion by siRNA did not inhibit the repression of HIPK2 by ADR (see Fig. S5C in the supplemental material). These data suggest that the N-terminal region of HIPK2, but not the C-terminal region, is necessary for SCF^{Fbx3}-induced degradation. Although we were unable to identify which lysine residue(s) is necessary for ubiquitination and degradation by SCF^{Fbx3}, it appears that HIPK2 degradation by SCF^{Fbx3} is different from MDM2-induced degradation and does not require lysine 25.

The degradation of p300 via the 26S proteasome pathway has previously been reported (6, 36, 48). This degradation appears to be dependent on p300 phosphorylation and dephosphorylation (9, 47). Doxorubicin-activated p38 mitogen-activated protein kinase phosphorylates p300 and induces p300 degradation (47). Protein phosphatase 2A, a serine-threonine phosphatase, also plays an important role in p300 degradation (9). Our data show that p300 is degraded by SCF^{Fbx3} via the 26S proteasome pathway, although it is unclear which modification of p300 mediates this degradation. Nonetheless, Fbx3

interacted with a form of p300 that had a faster electrophoretic mobility on SDS-polyacrylamide gels in the presence of MG132 (data not shown), suggesting that SCF^{Fbx3} recognizes and degrades dephosphorylated p300.

PML stimulates transcription by stabilizing HIPK2 and p300. PML has been suggested to play a role in the transcription of target genes that are regulated by transcription factors such as p53. However, the underlying mechanism has remained unclear. Our results suggest that PML stimulates transcription by protecting transcription coactivators such as HIPK2 and p300 from proteasome-dependent degradation. We demonstrated that PML inhibits the degradation of HIPK2 and p300 by the ubiquitin-proteasome pathway (Fig. 5A and B) and that this inhibition occurs in NBs (Fig. 5E). PML has been suggested to increase protein stability. For instance, PML enhances p53 stability by sequestering MDM2 in the nucleolus (4) and inhibits p73 ubiquitin-dependent degradation (5, 45). These reports are in agreement with our data showing that PML increases protein stability. In particular, the colocalization of PML in NBs is required for the stabilization of HIPK2, p300, and p73. In contrast, other groups have shown that NBs act as sites for proteasomal protein degradation by recruiting subunits of proteasomes and ubiquitin (2, 34, 35). However, these studies showed only that the ubiquitin-proteasome pathway-related proteins were recruited to NBs. There has been no report showing that proteasomal protein degradation actually occurs in NBs. Therefore, we suggest that PML may regulate protein stability by inhibiting protein degradation within NBs, while still allowing protein degradation by the ubiquitin-proteasome pathway to occur around the outside of NBs. In fact, the components of SCF^{Fbx3} which are essential for the degradation of HIPK2 and p300 were localized at the peripheries of NBs (Fig. 1C). In this way, it would be possible to finely regulate protein stability/degradation at the peripheries of NBs. Thus, it is not surprising in this respect that the proteins linked to degradation, proteasome subunits, and ubiquitin are found in NBs. As for the site of proteasomal protein degradation, Mattsson and coworkers showed that NB-associated proteins move to the nucleolus in the presence of MG132 and that the nucleolus may regulate proteasomal protein degradation (40). In the present study, we detected HIPK2 and p300 outside of NBs in the presence of MG132 but failed to detect PML, HIPK2, or p300 in the nucleolus (Fig. 5E). Although further studies concerning the actual site of proteasomal protein degradation will be required, it is clear from the work presented here and elsewhere that PML is crucial for the ubiquitin-proteasome pathway.

As shown in Fig. 3A, Fbx3 and PML cooperatively activated p53-dependent transcription, and Fbx3 was required for the enhanced transcription activity of p53 mediated by PML (Fig. 3B and C). Furthermore, Fbx3 and PML synergistically enhanced the HIPK2-stimulated transcriptional activity of p53 (Fig. 6B). Since PML stabilized HIPK2 ubiquitinated by Fbx3 (Fig. 6A), these results suggest that the ubiquitination of HIPK2 stimulates the transcriptional activity of p53. Important roles for ubiquitin in transcriptional regulation have been reported (10). The F-box protein Skp2 induces the ubiquitination and degradation of c-Myc but upregulates c-Myc transcriptional activity (29, 55). Likewise, the E3 ubiquitin ligases RSP5 and E6-AP activate hormone receptor-dependent transcription (25, 43), and SCF^{Met30}-induced ubiquitination of VP16 appears to be essential for transcriptional activation (51). Taken together, these findings indicate that stabilizing ubiquitinated HIPK2 appears to upregulate the transcriptional activity of p53 as shown in Fig. 6B. We speculate that ubiquitinated HIPK2 could activate p53-dependent transcription by increasing the phosphorylation of p300 and p53. It is also possible that ubiquitinated HIPK2 and p300 are degraded rapidly after the completion of the transcription of their target genes to ensure the complete shutdown of transcription. The regulation of the exact timing and levels of transcription in this way could constitute a novel mechanism for regulating gene expression.

Dysfunction of HIPK2 and p300 in leukemia pathogenesis. It has been reported that the PML-RARα fusion, which is generated by the chromosome translocation t(15;17) found for APL, forms stable oligomers with normal PML and inhibits PML-mediated transcriptional activation in a dominant-negative manner. We have shown here that PML and PML-RARα play opposite roles in HIPK2 stability (Fig. 7A to D). This may be because PML-RARα disrupts NBs, in which HIPK2 is stabilized as shown in Fig. 5A and E. The result showing that removal of the Fbx3-interacting region of PML-RARα destabilized HIPK2 (see Fig. S4 in the supplemental material) also suggests that the disruption of NBs by PML-RARα decreases protein stability. As PML-RARα enhanced HIPK2 degradation, PML-RARα would repress transcription by destabilizing coactivators such as HIPK2 and p300, perhaps contributing in this way to the pathogenesis of leukemia. Mutations in HIPK2 and p300 have been found for acute myeloid leukemia (AML) and myelodysplastic syndrome. p300 is involved in chromosome translocations such as t(8;22) and t(11;22) found in AML (8, 23, 31). We have recently found mutations in the *HIPK2* gene in association with AML and myelodysplastic syndrome that impair p53- and AML1-mediated transcription (37). These results suggest that dysfunctions of HIPK2 and p300 may be implicated in leukemia.

In summary, we propose that transcription is regulated by SCF^{Fbx3} and PML, as shown in Fig. 7F. According to this model, PML would activate transcription by counteracting the degradation of the transcription coactivators HIPK2 and p300, whose degradation by the ubiquitin-proteasome pathway is mediated by the novel SCF^{Fbx3} ubiquitin ligase. Conversely, PML-RARα would inactivate transcription by blocking the function of PML, thereby enhancing the SCF^{Fbx3}-induced degradation of HIPK2.

ACKNOWLEDGMENTS

We thank Y. Taya (National Cancer Center Research Institute) for kindly providing the cDNAs for p53 cDNA and the MDM2-luc reporter. We also thank Yukiko Aikawa, Noriko Aikawa, and Chikako Hatanaka for technical assistance.

This work was supported in part by grants-in-aid for scientific research from the Ministry of Health, Labor and Welfare and from the Ministry of Education, Culture, Sports, Science and Technology and by the Program for Promotion of Fundamental Studies from the National Institute of Biomedical Innovation of Japan.

REFERENCES

1. **Aikawa, Y., L. A. Nguyen, K. Isono, N. Takakura, Y. Tagata, M. L. Schmitz, H. Koseki, and I. Kitabayashi.** 2006. Roles of HIPK1 and HIPK2 in AML1- and p300-dependent transcription, hematopoiesis and blood vessel formation. EMBO J. **25:**3955–3965.

2. **Anton, L. C., U. Schubert, I. Bacik, M. F. Principiotta, P. A. Wearsch, J. Gibbs, P. M. Day, C. Realini, M. C. Rechsteiner, J. R. Bennink, and J. W. Yewdell.** 1999. Intracellular localization of proteasomal degradation of a viral antigen. J. Cell Biol. **146:**113–124.
3. **Avantaggiati, M. L., V. Ogryzko, K. Gardner, A. Giordano, A. S. Levine, and K. Kelly.** 1997. Recruitment of p300/CBP in p53-dependent signal pathways. Cell **89:**1175–1184.
4. **Bernardi, R., P. P. Scaglioni, S. Bergmann, H. F. Horn, K. H. Vousden, and P. P. Pandolfi.** 2004. PML regulates p53 stability by sequestering Mdm2 to the nucleolus. Nat. Cell Biol. **6:**665–672.
5. **Bernassola, F., P. Salomoni, A. Oberst, C. J. Di Como, M. Pagano, G. Melino, and P. P. Pandolfi.** 2004. Ubiquitin-dependent degradation of p73 is inhibited by PML. J. Exp. Med. **199:**1545–1557.
6. **Brouillard, F., and C. E. Cremisi.** 2003. Concomitant increase of histone acetyltransferase activity and degradation of p300 during retinoic acid-induced differentiation of F9 cells. J. Biol. Chem. **278:**39509–39516.
7. **Cenciarelli, C., D. S. Chiaur, D. Guardavaccaro, W. Parks, M. Vidal, and M. Pagano.** 1999. Identification of a family of human F-box proteins. Curr. Biol. **9:**1177–1179.
8. **Chaffanet, M., L. Gressin, C. Preudhomme, V. Soenen-Cornu, D. Birnbaum, and M. J. Pebusque.** 2000. MOZ is fused to p300 in an acute monocytic leukemia with t(8;22). Genes Chromosomes Cancer **28:**138–144.
9. **Chen, J., J. R. St-Germain, and Q. Li.** 2005. B56 regulatory subunit of protein phosphatase 2A mediates valproic acid-induced p300 degradation. Mol. Cell. Biol. **25:**525–532.
10. **Conaway, R. C., C. S. Brower, and J. W. Conaway.** 2002. Emerging roles of ubiquitin in transcription regulation. Science **296:**1254–1258.
11. **de The, H., C. Chomienne, M. Lanotte, L. Degos, and A. Dejean.** 1990. The t(15;17) translocation of acute promyelocytic leukaemia fuses the retinoic acid receptor alpha gene to a novel transcribed locus. Nature **347:**558–561.
12. **de The, H., C. Lavau, A. Marchio, C. Chomienne, L. Degos, and A. Dejean.** 1991. The PML-RAR alpha fusion mRNA generated by the t(15;17) translocation in acute promyelocytic leukemia encodes a functionally altered RAR. Cell **66:**675–684.
13. **D'Orazi, G., B. Cecchinelli, T. Bruno, I. Manni, Y. Higashimoto, S. Saito, M. Gostissa, S. Coen, A. Marchetti, G. Del Sal, G. Piaggio, M. Fanciulli, E. Appella, and S. Soddu.** 2002. Homeodomain-interacting protein kinase-2 phosphorylates p53 at Ser 46 and mediates apoptosis. Nat. Cell Biol. **4:**11–19.
14. **Dyck, J. A., G. G. Maul, W. H. Miller, Jr., J. D. Chen, A. Kakizuka, and R. M. Evans.** 1994. A novel macromolecular structure is a target of the promyelocyte-retinoic acid receptor oncoprotein. Cell **76:**333–343.
15. **Fogal, V., M. Gostissa, P. Sandy, P. Zacchi, T. Sternsdorf, K. Jensen, P. P. Pandolfi, H. Will, C. Schneider, and G. Del Sal.** 2000. Regulation of p53 activity in nuclear bodies by a specific PML isoform. EMBO J. **19:**6185–6195.
16. **Gilliland, D. G.** 1998. Molecular genetics of human leukemia. Leukemia **12**(Suppl. 1)**:**S7–S12.
17. **Glickman, M. H., and A. Ciechanover.** 2002. The ubiquitin-proteasome proteolytic pathway: destruction for the sake of construction. Physiol. Rev. **82:**373–428.
18. **Goddard, A. D., J. Borrow, P. S. Freemont, and E. Solomon.** 1991. Characterization of a zinc finger gene disrupted by the t(15;17) in acute promyelocytic leukemia. Science **254:**1371–1374.
19. **Gresko, E., A. Moller, A. Roscic, and M. L. Schmitz.** 2005. Covalent modification of human homeodomain interacting protein kinase 2 by SUMO-1 at lysine 25 affects its stability. Biochem. Biophys. Res. Commun. **329:**1293–1299.
20. **Guo, A., P. Salomoni, J. Luo, A. Shih, S. Zhong, W. Gu, and P. P. Pandolfi.** 2000. The function of PML in p53-dependent apoptosis. Nat. Cell Biol. **2:**730–736.
21. **Haupt, Y., R. Maya, A. Kazaz, and M. Oren.** 1997. Mdm2 promotes the rapid degradation of p53. Nature **387:**296–299.
22. **Hofmann, T. G., A. Moller, H. Sirma, H. Zentgraf, Y. Taya, W. Droge, H. Will, and M. L. Schmitz.** 2002. Regulation of p53 activity by its interaction with homeodomain-interacting protein kinase-2. Nat. Cell Biol. **4:**1–10.
23. **Ida, K., I. Kitabayashi, T. Taki, M. Taniwaki, K. Noro, M. Yamamoto, M. Ohki, and Y. Hayashi.** 1997. Adenoviral E1A-associated protein p300 is involved in acute myeloid leukemia with t(11;22)(q23;q13). Blood **90:**4699–4704.
24. **Ilyin, G. P., M. Rialland, C. Pigeon, and C. Guguen-Guillouzo.** 2000. cDNA cloning and expression analysis of new members of the mammalian F-box protein family. Genomics **67:**40–47.
25. **Imhof, M. O., and D. P. McDonnell.** 1996. Yeast RSP5 and its human homolog hRPF1 potentiate hormone-dependent activation of transcription by human progesterone and glucocorticoid receptors. Mol. Cell. Biol. **16:**2594–2605.
26. **Isono, K., K. Nemoto, Y. Li, Y. Takada, R. Suzuki, M. Katsuki, A. Nakagawara, and H. Koseki.** 2006. Overlapping roles for homeodomain-interacting protein kinases Hipk1 and Hipk2 in the mediation of cell growth in response to morphogenetic and genotoxic signals. Mol. Cell. Biol. **26:**2758–2771.
27. **Jensen, K., C. Shiels, and P. S. Freemont.** 2001. PML protein isoforms and the RBCC/TRIM motif. Oncogene **20:**7223–7233.
28. **Kakizuka, A., W. H. Miller, Jr., K. Umesono, R. P. Warrell, Jr., S. R. Frankel, V. V. Murty, E. Dmitrovsky, and R. M. Evans.** 1991. Chromosomal translocation t(15;17) in human acute promyelocytic leukemia fuses RAR alpha with a novel putative transcription factor, PML. Cell **66:**663–674.
29. **Kim, S. Y., A. Herbst, K. A. Tworkowski, S. E. Salghetti, and W. P. Tansey.** 2003. Skp2 regulates Myc protein stability and activity. Mol. Cell **11:**1177–1188.
30. **Kipreos, E. T., and M. Pagano.** 2000. The F-box protein family. Genome Biol. **1:**REVIEWS3002.
31. **Kitabayashi, I., Y. Aikawa, A. Yokoyama, F. Hosoda, M. Nagai, N. Kakazu, T. Abe, and M. Ohki.** 2001. Fusion of MOZ and p300 histone acetyltransferases in acute monocytic leukemia with a t(8;22)(p11;q13) chromosome translocation. Leukemia **15:**89–94.
32. **Kitabayashi, I., A. Yokoyama, K. Shimizu, and M. Ohki.** 1998. Interaction and functional cooperation of the leukemia-associated factors AML1 and p300 in myeloid cell differentiation. EMBO J. **17:**2994–3004.
33. **Kubbutat, M. H., S. N. Jones, and K. H. Vousden.** 1997. Regulation of p53 stability by Mdm2. Nature **387:**299–303.
34. **Lafarga, M., M. T. Berciano, E. Pena, I. Mayo, J. G. Castano, D. Bohmann, J. P. Rodrigues, J. P. Tavanez, and M. Carmo-Fonseca.** 2002. Clastosome: a subtype of nuclear body enriched in 19S and 20S proteasomes, ubiquitin, and protein substrates of proteasome. Mol. Biol. Cell **13:**2771–2782.
35. **Lallemand-Breitenbach, V., J. Zhu, F. Puvion, M. Koken, N. Honore, A. Doubeikovsky, E. Duprez, P. P. Pandolfi, E. Puvion, P. Freemont, and H. de The.** 2001. Role of promyelocytic leukemia (PML) sumolation in nuclear body formation, 11S proteasome recruitment, and As2O3-induced PML or PML/retinoic acid receptor alpha degradation. J. Exp. Med. **193:**1361–1371.
36. **Li, Q., A. Su, J. Chen, Y. A. Lefebvre, and R. J. Hache.** 2002. Attenuation of glucocorticoid signaling through targeted degradation of p300 via the 26S proteasome pathway. Mol. Endocrinol. **16:**2819–2827.
37. **Li, X. L., Y. Arai, H. Harada, Y. Shima, H. Yoshida, S. Rokudai, Y. Aikawa, A. Kimura, and I. Kitabayashi.** 2007. Mutations of the HIPK2 gene in acute myeloid leukemia and myelodysplastic syndrome impair AML1- and p53-mediated transcription. Oncogene **26:**7231–7239.
38. **Lill, N. L., S. R. Grossman, D. Ginsberg, J. DeCaprio, and D. M. Livingston.** 1997. Binding and modulation of p53 by p300/CBP coactivators. Nature **387:**823–827.
39. **Look, A. T.** 1997. Oncogenic transcription factors in the human acute leukemias. Science **278:**1059–1064.
40. **Mattsson, K., K. Pokrovskaja, C. Kiss, G. Klein, and L. Szekely.** 2001. Proteins associated with the promyelocytic leukemia gene product (PML)-containing nuclear body move to the nucleolus upon inhibition of proteasome-dependent protein degradation. Proc. Natl. Acad. Sci. USA **98:**1012–1017.
41. **Miyoshi, H., K. Shimizu, T. Kozu, N. Maseki, Y. Kaneko, and M. Ohki.** 1991. t(8;21) breakpoints on chromosome 21 in acute myeloid leukemia are clustered within a limited region of a single gene, AML1. Proc. Natl. Acad. Sci. USA **88:**10431–10434.
42. **Moller, A., H. Sirma, T. G. Hofmann, S. Rueffer, E. Klimczak, W. Droge, H. Will, and M. L. Schmitz.** 2003. PML is required for homeodomain-interacting protein kinase 2 (HIPK2)-mediated p53 phosphorylation and cell cycle arrest but is dispensable for the formation of HIPK domains. Cancer Res. **63:**4310–4314.
43. **Nawaz, Z., D. M. Lonard, C. L. Smith, E. Lev-Lehman, S. Y. Tsai, M. J. Tsai, and B. W. O'Malley.** 1999. The Angelman syndrome-associated protein, E6-AP, is a coactivator for the nuclear hormone receptor superfamily. Mol. Cell. Biol. **19:**1182–1189.
44. **Nguyen, L. A., P. P. Pandolfi, Y. Aikawa, Y. Tagata, M. Ohki, and I. Kitabayashi.** 2005. Physical and functional link of the leukemia-associated factors AML1 and PML. Blood **105:**292–300.
45. **Oberst, A., M. Rossi, P. Salomoni, P. P. Pandolfi, M. Oren, G. Melino, and F. Bernassola.** 2005. Regulation of the p73 protein stability and degradation. Biochem. Biophys. Res. Commun. **331:**707–712.
46. **Pearson, M., R. Carbone, C. Sebastiani, M. Cioce, M. Fagioli, S. Saito, Y. Higashimoto, E. Appella, S. Minucci, P. P. Pandolfi, and P. G. Pelicci.** 2000. PML regulates p53 acetylation and premature senescence induced by oncogenic Ras. Nature **406:**207–210.
47. **Poizat, C., P. L. Puri, Y. Bai, and L. Kedes.** 2005. Phosphorylation-dependent degradation of p300 by doxorubicin-activated p38 mitogen-activated protein kinase in cardiac cells. Mol. Cell. Biol. **25:**2673–2687.
48. **Poizat, C., V. Sartorelli, G. Chung, R. A. Kloner, and L. Kedes.** 2000. Proteasome-mediated degradation of the coactivator p300 impairs cardiac transcription. Mol. Cell. Biol. **20:**8643–8654.
49. **Rabbitts, T. H.** 1994. Chromosomal translocations in human cancer. Nature **372:**143–149.
50. **Rinaldo, C., A. Prodosmo, F. Mancini, S. Iacovelli, A. Sacchi, F. Moretti, and S. Soddu.** 2007. MDM2-regulated degradation of HIPK2 prevents p53Ser46 phosphorylation and DNA damage-induced apoptosis. Mol. Cell **25:**739–750.
51. **Salghetti, S. E., A. A. Caudy, J. G. Chenoweth, and W. P. Tansey.** 2001.

Regulation of transcriptional activation domain function by ubiquitin. Science **293:**1651–1653.
52. **Salomoni, P., and P. P. Pandolfi.** 2002. The role of PML in tumor suppression. Cell **108:**165–170.
53. **Takahashi, Y., V. Lallemand-Breitenbach, J. Zhu, and H. de The.** 2004. PML nuclear bodies and apoptosis. Oncogene **23:**2819–2824.
54. **Tanaka, K., T. Suzuki, N. Hattori, and Y. Mizuno.** 2004. Ubiquitin, proteasome and parkin. Biochim. Biophys. Acta **1695:**235–247.
55. **von der Lehr, N., S. Johansson, S. Wu, F. Bahram, A. Castell, C. Cetinkaya, P. Hydbring, I. Weidung, K. Nakayama, K. I. Nakayama, O. Soderberg, T. K. Kerppola, and L. G. Larsson.** 2003. The F-box protein Skp2 participates in c-Myc proteosomal degradation and acts as a cofactor for c-Myc-regulated transcription. Mol. Cell **11:**1189–1200.
56. **Wang, Z. G., D. Ruggero, S. Ronchetti, S. Zhong, M. Gaboli, R. Rivi, and P. P. Pandolfi.** 1998. PML is essential for multiple apoptotic pathways. Nat. Genet. **20:**266–272.
57. **Yoshida, H., H. Ichikawa, Y. Tagata, T. Katsumoto, K. Ohnishi, Y. Akao, T. Naoe, P. P. Pandolfi, and I. Kitabayashi.** 2007. PML-retinoic acid receptor α inhibits PML IV enhancement of PU.1-induced C/EBPε expression in myeloid differentiation. Mol. Cell. Biol. **27:**5819–5834.
58. **Zhong, S., P. Salomoni, and P. P. Pandolfi.** 2000. The transcriptional role of PML and the nuclear body. Nat. Cell Biol. **2:**E85–E90.

Review Article

Roles of the histone acetyltransferase monocytic leukemia zinc finger protein in normal and malignant hematopoiesis

Takuo Katsumoto, Naomi Yoshida and Issay Kitabayashi[1]

Molecular Oncology Division, National Cancer Center Research Institute, 5-1-1 Tsukiji, Chuo-ku, Tokyo, 104-0045, Japan

(Received March 18, 2008/Revised April 17, 2008/Accepted April 20, 2008/Online publication July 29, 2008)

Histone-modified enzymes are involved in various cell functions, including proliferation, differentiation, cell death and carcinogenesis. The protein MOZ (monocytic leukemia zinc finger protein) is a Myst (MOZ, Ybf2 (Sas3), Sas2, Tip60)-type histone acetyltranseferase (HAT) that generates fusion genes, such as *MOZ–TIF2, MOZ–CBP* and *MOZ–p300*, in acute myeloid leukemia (AML) by chromosomal translocation. MOZ associates with AML1 (RUNX1), PU.1, and p53, and cooperatively activates target gene transcription. Gene targeting in mice has revealed that MOZ is essential for the generation and maintenance of hematopoietic stem cells (HSC) and for the appropriate development of myeloid, erythroid and B-lineage cell progenitors. In AML, *MOZ* fusion genes lead to repressed differentiation, hyper-proliferation, and self-renewal of myeloid progenitors through deregulation of MOZ-regulated target gene expression. It is therefore necessary to analyze the roles of MOZ and MOZ fusion genes in normal and malignant hematopoiesis to elucidate the mechanisms underlying and develop therapies for MOZ-related AML. (*Cancer Sci* 2008; 99: 1523–1527)

In acute myeloid leukemia (AML), fusion genes often form as the result of specific chromosomal translocations.[1,2] Many of these fused genes, including *MOZ*, are transcription-related factors involved in the development or self-renewal of hematopoietic stem cells (HSC) and/or in hematopoietic cell differentiation.[3,4] Monocytic leukemia zinc finger protein (MOZ) is a Myst (MOZ, Ybf2 (Sas3), Sas2, Tip60)-type histone acetyltranseferase (HAT) that functions as a transcriptional coactivator for hematopoietic transcription factors such as AML1.[5,6] Recently, we and others used gene-targeted mice to reveal critical roles for MOZ in hematopoiesis, particularly in the self-renewal of HSC.[7,8] *MOZ* fusion genes can also transform HSC and myeloid progenitor cells into leukemia cells and confer unto them self-renewal activity.[9,10] Researching the functions of *MOZ* and *MOZ* fusion genes in normal and malignant hematopoiesis can aid in understanding the mechanisms of AML development and leukemic cell-renewal activity. Such discoveries may allow the development of improved AML therapies.

Involvement of the *MOZ* gene in chromosomal translocations

Chromosomal translocations, which are frequently detected in patients with AML, include t(8;21), inv(16), t(15;17) and t(11; v) (v: variable) result in the gene fusions *AML1–ETO, CBFβ–MYH11, PML–RARα* and *MLL*-fusions, respectively. *MOZ* was first identified as a gene involved in the translocation t(8;16)(p11;p13) resulting in the *MOZ–CBP* fusion gene.[11] The *MOZ–p300, MOZ–TIF2* and *MOZ–NcoA3* fusion genes were later identified in AML from t(8;22)(p11;q13),[12,13] inv(8)(p11;q13)[14,15] and t(8; 20)(p11;q13),[16] respectively (Fig. 1). *MOZ* is also involved in a patient of pediatric therapy-related myelodysplastic syndrome with a novel chromosomal translocation t(2;8)(p23;p11).[17] *MOZ-related factor (MORF; Myst4, Querkopf)*, a HAT that is highly homologous to *MOZ*,[18,19] also generates fusion genes with *CBP* and probably also with *Gcn5* in various disorders, including AML[20,21] therapy-related myelodysplastic syndrome[22] and uterine leiomyomata.[23]

All *MOZ* fusion partner genes are involved in histone modification and transcriptional regulation. CBP and p300 are major HAT[24] that function as coactivators for various transcription factors. TIF2 (NcoA2/GRIP1) and NcoA3 (TRAM-1/RAC3/pCIP/AIB-1) are adaptor proteins that combine nuclear receptors with CBP.[25] AML that express MOZ fusion genes are typically monocytic leukemias classified as M4/M5 among French–American–British (FAB) subtypes;[18] MOZ-related translocation is found in about 6.5% of such AML subtypes.[16]

In all *MOZ* fusion genes, breakpoints of MOZ are located in or around its acidic domain (Fig. 1). As a result, the N-terminal region of MOZ is retained and the C-terminal region is replaced with the fusion partners, such as CBP or p300. The N-terminal region of MOZ contains a H15 (histone H1/H5) domain related to nuclear localization,[5] a PHD (plant homeobox-like domain) zinc finger involved in binding to methylated histone, a basic domain and a Myst-type HAT domain. The HAT domain contains a C_2HC zinc finger and helix–turn–helix motifs that bind to nucleosomes[26] and DNA.[27] Taken together, these structures suggest that *MOZ* fusion genes may affect the transcription of MOZ target genes with deregulated acetylation states.

HAT activity and transcriptional regulation

Histone acetylation is one of the major epigenetic mechanisms to regulate gene expression.[28] MOZ is capable of acetylating histones H2A and H3 at K14, and H4 at K5, 8, 12, and 16 *in vitro*.[5,6] Five Myst-type acetyltransferases are known in humans: MOF (Myst1); HBO1(Myst2); MOZ (Myst3); MORF (Myst4); and TIP60.[29] With the exception of MOF, all of the Myst-type acetyltransferases are involved in transcriptional complexes with inhibition of growth (ING) family proteins.[30,31] MOZ and MORF form the yeast NuA3-like transcriptional complex with ING5, BRPF1/2/3 and hEaf6. The yeast NuA3 complex aids the acetylation of histone H3 at K14, which is associated with transcription and replication.[31]

[1]To whom correspondence should be addressed. E-mail: ikitabay@ncc.go.jp

doi: 10.1111/j.1349-7006.2008.00865.x

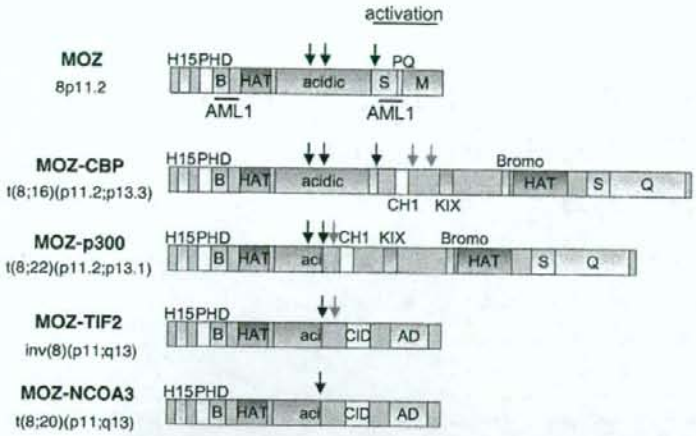

Fig. 1. Structure of normal monocytic leukemia zinc finger protein (MOZ) and leukemia-associated MOZ fusion proteins. MOZ has various functional domains including H1/5 (H15; histone H1/H5-like), PHD (plant homeobox-like domain) zinc finger, B basic (b), histone acetyltranseferase (HAT) and acidic domains. S, PQ and M indicate serine-, proline- and glutamine-, and methionine-rich domains, respectively. MOZ fusions with four known partners are shown: CBP, p300, TIF2 and the recently identified NCOA3. MOZ fusion partners contained CH1 (cystein/histidine rich domain 1), KIX (kinase-inducible) domain, Bromodomain (Bromo), CID (CBP interacting domain) and AD (activation domain). The breakpoints in the MOZ gene and its fusion partners are shown as black arrows and blue arrows, respectively.

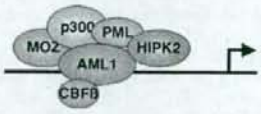

Fig. 2. Role of monocytic zinc finger protein (MOZ) in acute myeloid leukemia (AML)1-dependent transcription. AML1 acts as both a sequence-specific transacting factor and a scaffold to intermediate the association of HIPK2 and histone acetyltranseferase (HAT). MOZ functions as coactivator for AML1 and activicates AML1-mediated transcription.

MOZ specifically interacts with transcription factors such as AML1,[5] PU.1,[8] p53, Runx2[32] and NF-κB,[33] functioning as their transcriptional coactivator. AML1 forms large multiprotein complexes including CBFβ as a 'core component' as well as several classes of chromatin modulators such as p300 or CBP,[34] MOZ,[13] PML[35] and HIPK2[36] as a 'regulatory complex' (Fig. 2).[37] MOZ cooperatively activates AML1-dependent transcription of genes such as *MPO (myeloperoxidase)*[5] or *macrophage inflammatory protein (MIP)-1α*.[38] Interaction of MOZ with Runx2[32], p65/NF-κB[33] or p53 (S. R. and I. K., unpublished data) can activate their transcription factor-dependent gene expression. The role of HAT activity in MOZ function remains unclear. For instance, the HAT domain of MOZ is required for NF-κB-dependent transcription[33] but not for AML1-mediated transcription,[5] suggesting target-dependent roles for HAT activity in transcriptional regulation. The leukemia-associated fusion protein MOZ–CBP inhibits AML1-dependent activation of the *MPO* promoter[5] but activates NF-κB-dependent transcription.[33] These results indicate that effects of MOZ fusion proteins on transcription are dependent on promoter contexts.

During hepatocarcinogenesis, MOZ activates MafK and Nrf2-dependent transcription of the *GSTP* gene.[39] In moz mutant zebrafish, hoxa2b and hoxb2a expression is lost and the support skeleton of the second pharyngeal segment is transformed into a mirror-image duplicated jaw skeleton.[40,41] Defective Hox gene expression in *moz* mutants is partially recovered by the histone deacetylase inhibitor trichostatin A. Consistent with moz-deficient zebrafish, HoxA9 expression is also decreased in hematopoietic cells in *MOZ*-deficient mice.[8] Additionally, expression of HoxA9, HoxA10 and Meis1 are increased in AML patients with *MOZ* fusion genes.[42] These results indicate that MOZ-regulated genes are involved in development, hematopoiesis and carcinogenesis.

Roles of MOZ in hematopoiesis

MOZ cooperatively activates target genes of AML1 and PU.1 that play important roles in hematopoiesis.[5,8] We previously demonstrated that MOZ-deficient mice are embryonic lethal at E15 with a pale appearance and a small liver, the major organ that produces hematopoietic cells at this period.[8] These mice have significantly decreased production of mature erythrocytes; the embryonic lethal state likely results from defective erythrocyte maturation around E15, because primitive erythrocytes are exchanged with definitive erythrocytes during this period.

Cell numbers in MOZ-deficient fetal livers are about half those of wild-type animals. MOZ-deficient hematopoietic progenitor cells produce colonies on methylcellulose medium with appropriate cytokines with cell numbers of one-fifth to one-tenth those of wild-type cells. HSC and their progenitors are severely decreased in MOZ-deficient fetal livers, and $CD19^+$ B-lineage cells are also significantly decreased. In contrast, populations of granulocytes and monocytes, as well as myeloid progenitor KLSF ($c\text{-}Kit^+$, Lin^-, $Sca\text{-}1^-$, $FcR\gamma^+$), the population of which is small in normal fetal liver and bone marrow, are increased in MOZ-deficient fetal liver. KLSF cells in normal and MOZ-deficient fetal liver can form myeloid colonies in methylcellulose medium and differentiate into either granulocytes or monocytes *in vitro*. Increases in the committed myeloid cells suggest that myeloid differentiation is inhibited around the KLSF stage in $MOZ^{(-/-)}$ mice, because MOZ has important roles in the regulation of this stage. Taken together, these results indicate that MOZ plays key roles for appropriate development and differentiation of lymphoid and myeloid cells (Fig. 3).

MOZ is also required for self-renewal of hematopoietic stem cells. When MOZ-deficient fetal liver cells are transplanted into irradiated mice, recipient mice do not develop a reconstituted hematopoietic system, even when excess numbers of fetal liver cells are transplanted. Gene expression analysis reveals that the expression of c-Kit, c-Mpl and HoxA9 is reduced in MOZ-deficient compared with wild-type mice. Thomas *et al.* reported the lethality at birth of mice with a MOZ C-terminal deletion (MOZ-ΔC mice)[7] a mouse model that is slightly different from the MOZ-deficient mice discussed above. Hematopoietic deficiency in MOZ-ΔC mice was observed in terms of decreased numbers of blood cells, significantly reduced hematopoietic progenitors (blasts) and HSC and an increase in nucleated erythrocytes. The HSC from these mice also have reduced CFU-S12 and hematopoietic reconstitution activities. Thymus T-cell development

doi: 10.1111/j.1349-7006.2008.00865.x

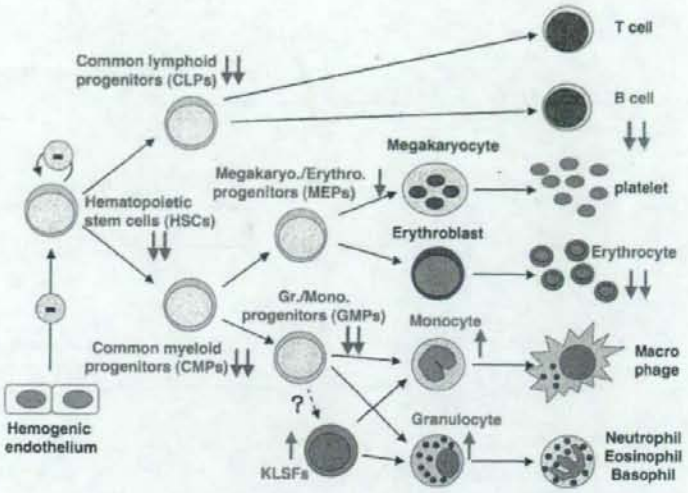

Fig. 3. Schematic for fetal hematopoiesis phenotypes of monocytic zinc finger protein (MOZ)-deficient mice. The MOZ-deficient fetal liver contains reduced hematopoietic progenitor and hematopoietic stem cells (HSC) have lost their self-renewal activity. Levels of $CD19^+$ B-lineage cells and mature erythrocytes are also severely reduced. In contrast, myeloid cell and KLSF ($c\text{-}Kit^+$, Lin^-, $Sca\text{-}1^-$, $FcR\gamma^+$) populations are increased in the MOZ-deficient fetal liver.

is normal, although thymocyte numbers are substantially reduced. On the other hand, the spleens of the MOZ-ΔC mice are critically affected.

As described above, MOZ interacts with AML1 and PU.1 transcription factors that have various functional roles in hematopoiesis. AML1-deficient mice display deficiencies in their ability to generate HSC, CLP (common lymphoid progenitors) and B cells and have an increased number of myeloid lineage cells.[43–46] PU.1-deficient mice display defects in CLP and most myeloid progenitor cells except MEP (megakaryo/erythroid progenitors).[47–49] MOZ-deficient mice show less severe phenotypes than either AML1- and PU.1-deficient mice, which is presumably because these transcription factors are not completely inactive in the absence of MOZ.[8] It is interesting that although the number of myeloid lineage cells is decreased in PU.1-null mice,[47] they are increased in PU.1 knockdown mice, as observed in MOZ-null mice.[50] These data suggest that part of the MOZ-deficient phenotype is due to the reduced activity of transcription factors.

Numerous studies have shown that HSC self-renewal activity is controlled by transcription modulating factors, signal transduction molecules or cell cycle regulators.[51,52] MOZ-deficient mice, in which HSC lose their self-renewal activity, display reduced expression of HoxA9,[53] c-Kit[54] and c-Mpl,[55,56] which are known to be involved in HSC self-renewal activity. Therefore, HSC dysfunction in MOZ-deficient mice results from the reduced expression of MOZ-target genes including *HoxA9*, *c-Kit*, and *c-Mpl*.

MOZ-associated leukemia and leukemic stem cells

The *MOZ* gene is involved in specific chromosomal translocations in monocytic leukemia. These translocations result in the expression of MOZ fusion proteins such as MOZ–CBP, MOZ–p300, MOZ–TIF2 and MOZ–NcoA3. It has been reported that MOZ–TIF2 can efficiently induce AML in mice after transplantation of HSC or myeloid progenitors in which *MOZ–TIF2* is introduced by retroviral vectors.[9] It has also been suggested that MOZ–TIF2 confers self-renewal activity to committed progenitor cells.[57] Several regions of the *MOZ–TIF2 fusion* gene are necessary to give rise to AML, including the C_2HC zinc finger motif that is associated with nucleosome binding and the Myst domain (both of the MOZ-derived region), and the LXXLL motif that is related to CBP recruitment (of the TIF2 region).[9] The MOZ PHD finger and the acetyl-coenzyme A binding site that is indispensable for HAT activity contribute to, but are not essential for, AML development. In the MOZ–TIF2-induced AML mouse model, levels of myeloid progenitor populations, including GMP (granulocyte/monocyte progenitors) and KLSF, are substantially increased.[57] Myeloid progenitor KLSF are also elevated in MOZ-deficient mice.[8] These results suggest that MOZ dysfunction is associated with AML induction by MOZ–TIF2.

It is also worthwhile to note that a graded reduction of PU.1 induces myeloproliferative disorder (MPD) or AML in mice.[50] MOZ–CBP inhibits AML1-dependent activation of the *MPO* promoter[3] but activates NF-κB-dependent transcription.[33] MOZ–TIF2 also represses retinoic-acid-receptor- and p53-dependent transcription.[58] Therefore, MOZ fusion proteins differently regulate transcription of their targets, with transcription effects being largely dependent on the promoter context (Fig. 4).

Camos *et al.* previously reported the gene expression profiles of AML patients with a t(8; 16) MOZ-CBP translocation compared with those of AML patients carrying other translocations.[42] *Prolactin* and the proto-oncogene *RET* are specifically over-expressed in MOZ–CBP patients, as are the homeobox genes *HoxA9*, *A10* and *Meis1*. Overexpression of Hox genes are often observed in leukemia patients including those with *MLL* gene rearrangements.[59] However, other hox genes, such as HoxA3, A7, or HoxB5 are not elevated in MOZ–CBP patients. One can conclude that HoxA9 is a target gene for both normal MOZ and leukemia-associated MOZ fusion proteins, because its expression is impaired in MOZ-deficient hematopoietic cells. It will be necessary to analyze the transcriptional regulation of *HoxA9* by MOZ or MOZ fusion genes to reveal the molecular mechanisms underlying the development of MOZ-related AML.

Conclusions

MOZ is a Myst-type acetyltransferase that coordinately activates the target genes of hematopoiesis-essential transcription factors such as AML1 and PU.1. MOZ is also indispensable for hematopoietic cell development and HSC self-renewal. In acute